

(S)-4-(Difluoromethyl)-5-(4-(3-methylmorpholino)-6-morpholino-1,3,5-triazin-2-yl)pyridin-2-amine (PQR530), a Potent, Orally Bioavailable, and Brain-Penetrable Dual Inhibitor of Class I PI3K and mTOR Kinase

Denise Rageot,^{†,||} Thomas Bohnacker,^{†,||} Erhan Keles,[†] Jacob A. McPhail,[‡] Reece M. Hoffmann,[‡] Anna Melone,[†] Chiara Borsari,[†] Rohitha Sriramaratnam,[†] Alexander M. Sele,[†] Florent Beauflis,[†] Paul Hebeisen,[§] Dorian Fabbro,[§] Petra Hillmann,[§] John E. Burke,[‡] and Matthias P. Wymann^{*,†,||}

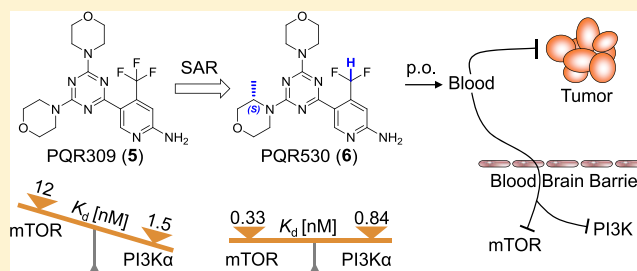
[†]Department of Biomedicine, University of Basel, Mattenstrasse 28, 4058 Basel, Switzerland

[‡]Department of Biochemistry and Microbiology, University of Victoria, Victoria, British Columbia V8W 2Y2, Canada

[§]PIQUR Therapeutics AG, Hochbergerstrasse 60C, 4057 Basel, Switzerland

Supporting Information

ABSTRACT: The phosphoinositide 3-kinase (PI3K)/mechanistic target of rapamycin (mTOR) pathway is frequently overactivated in cancer, and drives cell growth, proliferation, survival, and metastasis. Here, we report a structure–activity relationship study, which led to the discovery of a drug-like adenosine 5'-triphosphate-site PI3K/mTOR kinase inhibitor: (S)-4-(difluoromethyl)-5-(4-(3-methylmorpholino)-6-morpholino-1,3,5-triazin-2-yl)pyridin-2-amine (PQR530, compound 6), which qualifies as a clinical candidate due to its potency and specificity for PI3K and mTOR kinases, and its pharmacokinetic properties, including brain penetration. Compound 6 showed excellent selectivity over a wide panel of kinases and an excellent selectivity against unrelated receptor enzymes and ion channels. Moreover, compound 6 prevented cell growth in a cancer cell line panel. The preclinical *in vivo* characterization of compound 6 in an OVCAR-3 xenograft model demonstrated good oral bioavailability, excellent brain penetration, and efficacy. Initial toxicity studies in rats and dogs qualify 6 for further development as a therapeutic agent in oncology.



INTRODUCTION

The phosphoinositide 3-kinase (PI3K) mechanistic target of rapamycin (mTOR) signaling pathway plays a fundamental role in cell proliferation, growth, and survival. Aberrant activation of this signaling pathway has been shown to drive the progression of malignant tumors, which can be triggered by mutated growth factor receptors, PI3K, loss of PTEN (phosphatase and tensin homolog on chromosome 10), and effector proteins such as Ras.^{1–5} The resulting increase of cellular PtdIns(3,4,5)P₃ subsequently recruits protein kinase B (PKB/Akt), which is fully activated by phosphorylation by phosphoinositide-dependent kinase 1 and the TOR complex 2 (TORC2) kinase at the plasma membrane.⁴ By the phosphorylation of tuberous sclerosis 2 (TSC2, tuberin), PKB/Akt initiates the activation and assembly of TORC1 on endomembranes. TORC1 then augments cellular protein and lipid production via phosphorylation of S6 kinase (S6K). While TORC1 affects endomembrane dynamics and autophagy, TORC2 impacts on metabolic, cell cycle, and cytoskeletal changes.³

Drugs targeting the pathway at multiple nodes, such as the first dual PI3K/mTOR inhibitor BEZ235 (dactolisib),^{5,6} have

provided promising preclinical results attenuating tumor growth driven specifically by overactivated PI3K,⁷ but also block growth of cancer cells with multiple activated pathways, such as in melanoma.⁵ Although subsequent clinical studies of BEZ235 were plagued by adverse effects,⁸ dual PI3K/mTOR inhibitors are still considered a valuable asset in cancer therapy, and are pursued in clinical trials.²

Recently, we have presented PQR309 (bimiralisib, 5)^{9,10} as a novel, brain-penetrant pan-PI3K inhibitor, which also moderately targets mTOR kinase activity (Figure 1). First clinical results for 5 have been released,¹⁵ and the compound is currently in phase II clinical trials. To maximize potency, we focused on the development of a brain permeant follow-up compound with a major enhancement in mTOR kinase inhibition.

We analyzed the activity profiles of compounds with a similar structure and binding mode to 5 and assessed their *in vitro* dissociation constants (*K*_d) for class I PI3K isoforms (α , β , γ , and δ) and mTOR. A selection of relevant clinical

Received: March 26, 2019

Published: June 7, 2019

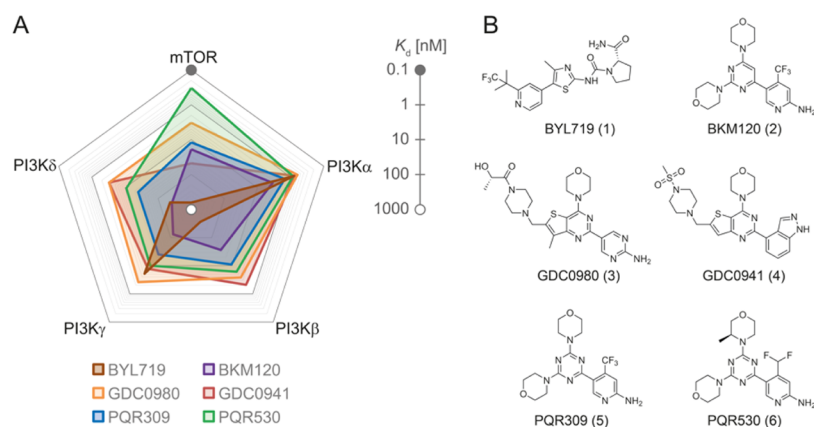
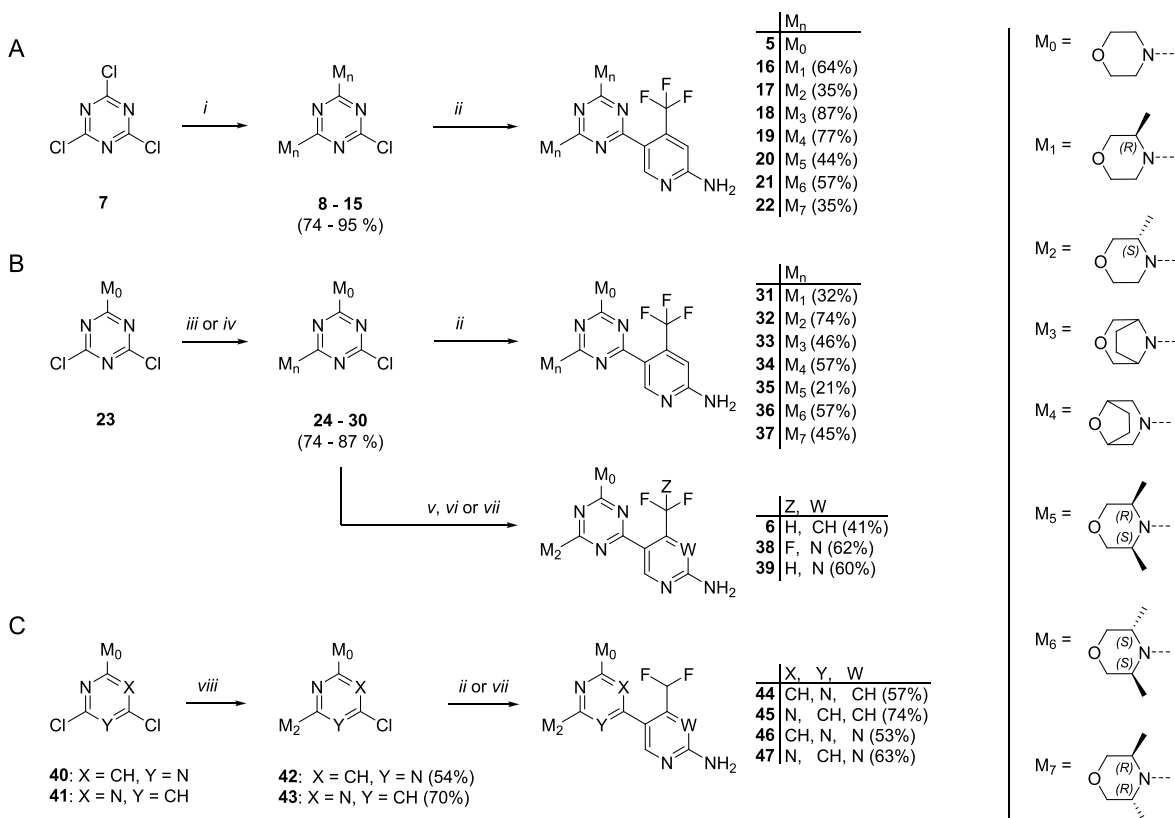


Figure 1. Affinity graph and chemical formulae of selected adenosine 5'-triphosphate (ATP)-competitive inhibitors for class I PI3K isoforms and mTOR kinase. (A) K_d values for each compound and kinase are presented as a radar diagram with reciprocal and logarithmic scaled axes. Data for compounds 2–5 are from ref 10. Dissociation constants (K_d) were determined using the ScanMax platform from DiscoverX;¹⁶ see Table S1, Supporting Information. (B) Chemical structure of clinically relevant selected compounds.

Scheme 1. Synthesis of Trisubstituted Triazine and Pyrimidine Core Compounds^a

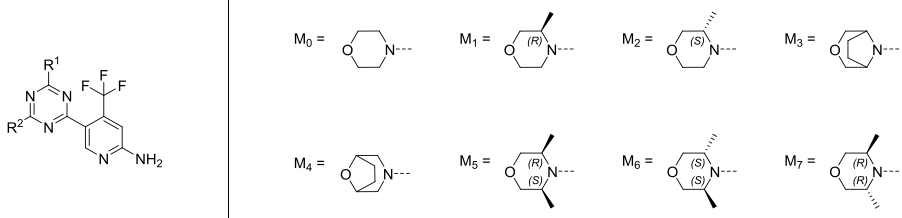


^aReagents and conditions: (i) morpholine derivative (M_n-H), CH_2Cl_2 , 0 °C \rightarrow room temperature (RT), o/n or as reported in the literature;¹⁷ (ii) (1) boronic acid pinacol ester (RBpin) 48 or 49, XPhos Pd G2 (cat.), K_3PO_4 , dioxane/ H_2O , 95 °C, 2–15 h; (2) HCl, H_2O , 60 °C, 3–15 h; (iii) M_n-H , N,N -diisopropylethylamine (DIPEA), EtOH, 0 °C \rightarrow RT, o/n; (iv) M_n-H , DIPEA, dioxane, 70 °C, o/n; (v) (1) Pd(OAc)₂/PPPh₃ (cat.), RBpin 49, K_2CO_3 , tetrahydrofuran (THF)/ H_2O , 55 °C, 2 h; (2) HCl, H_2O , 55 °C, o/n; (vi) RBpin, XPhos Pd G2 (cat.), K_3PO_4 , dioxane/ H_2O , 95 °C, 2 h; (vii) RBpin generated in situ (see the Supporting Information), XPhos Pd G2 (cat.), K_3PO_4 , dioxane/ H_2O , 95 °C, 3–5 h; (viii) M_n-H , DIPEA, 130 °C, o/n.

compounds is depicted in Figure 1 (for data, see Table S1 in the Supporting Information), and affinities for individual PI3K isoforms and mTOR provided a lead for novel compounds. Compound 1 (alpelisib, BYL719) has been reported as a specific PI3K α inhibitor,¹² but displayed in our hands only 7-fold selectivity over PI3K γ , while sparing PI3K β , PI3K δ , and mTOR (>250-fold). Pictilisib (GDC0941, 4)¹³ is a potent pan

class I inhibitor that strongly binds to PI3K α , β , and δ , with less affinity to PI3K γ ; however, its affinity to mTOR is >50-fold reduced compared to p110 α . All other compounds are to various degrees dual class I PI3K [PI3K isoforms (α , β , γ , and δ)] and mTOR kinase inhibitors: 2 (buparlisib, BKM120),^{9,14} 5,^{9–11,15} and 3 (apitolisib, GDC0980),¹³ which all target class I as well as mTOR. Compound 6 emerging from the study

Table 1. SAR Study of 4-(Trifluoromethyl)-5-(1,3,5-triazin-2-yl)pyridine-2-amines



cpd.	R ¹	R ²	cellular IC ₅₀ (nM) ^a		K _i (nM) ^b		K _i (p110α)/K _i (mTOR)	clogP ^c
			pPKB	pS6	p110α	mTOR		
PQR309 (5)	M ₀	M ₀	139	205	17	62	0.27	3.11
16	M ₁	M ₁	1702	1122	684	171	4.01	3.94
17	M ₂	M ₂	248	283	6.8	137	0.05	3.94
18	M ₃	M ₃	755	299	4643	76.8	60.5	4.04
19	M ₄	M ₄	947	691	731	177	4.12	4.04
20	M ₅	M ₅	567	437	31.4	39.6	0.79	4.76
21	M ₆	M ₆	610	531	37.0	265	0.14	4.76
22	M ₇	M ₇	>20 000	14 522	>20 000	1892	32.7	4.76
31	M ₀	M ₁	373	410	53.7	109	0.49	3.52
32	M ₀	M ₂	196	89.8	8.3	25.5	0.33	3.52
33	M ₀	M ₃	420	156	19.9	43.1	0.46	3.58
34	M ₀	M ₄	274	212	31.0	47.8	0.65	3.58
35	M ₀	M ₅	122	135	27.4	19.3	1.42	3.94
36	M ₀	M ₆	100	126	15.2	59.2	0.26	3.94
37	M ₀	M ₇	435	457	88.9	64.5	1.38	3.94

^aCellular phosphorylation of PKB/Akt on Ser473 and ribosomal S6 on Ser235/236 were analyzed in inhibitor-treated A2058 melanoma cells using in-cell western detection. Each experiment performed in triplicate or as a multiple of $n = 3$. ^bCompounds were tested in a time-resolved Förster resonance energy transfer (FRET-TR) assay (LanthaScreen), and inhibitor K_i s were calculated for PI3Kα and mTOR, as described in Experimental Section. The PI3Kα/mTOR column depicts the ratio of compound-specific PI3Kα K_i over the K_i for mTOR. Each experiment was performed at least twice or as a multiple of $n = 2$. ^cMarvin/JChem 16.10.17 was used for calculation of logP (partition coefficient) and polar surface area (PSA) values. For all compounds shown in this table, the calculated PSA values are equal to 102.5.

presented here is a subnanomolar inhibitor of PI3Kα and mTOR, and targets other class I PI3Ks at around 10 nM (Table S1). Here, we report the lead optimization process using 5 as a starting template to generate 6, a potent and brain-penetrant clinical candidate compound.

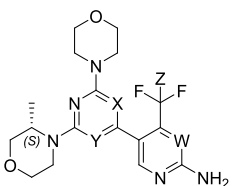
RESULTS AND DISCUSSION

Chemistry. To identify potent and dual PI3K/mTOR inhibitors with increased potency, selectivity, and brain distribution profile, a library of pyrimidine and triazine compounds were produced (Scheme 1). All triazine core compounds were prepared from cyanuric chloride (7), either via disubstitution by the same morpholine moiety (M_n, route A for symmetric compounds) or by subsequent substitution with two different morpholines (route B for asymmetric compounds). Depending on the morpholine substituent, this reaction yielded the intermediates in good to excellent yields (74–87%). The heteroaryl moieties were then introduced via Suzuki cross-coupling using the corresponding boronic acid pinacol ester. Boronic acid pinacol esters were either protected at their 2-amino group and isolated or generated in situ (see Experimental Section and the Supporting Information). The desired triazine core derivatives (5, 6, 16–22, and 31–39) were obtained in moderate to good yields (21–87%). The synthetic procedure for the preparation of pyrimidine core compounds (44–47) is depicted in route C. Similar to the synthesis of triazine derivatives, this synthesis involved a nucleophilic aromatic substitution, followed by a Suzuki cross-coupling reaction. The nucleophilic aromatic substitution of

2,4,6-trichloropyrimidine by an unsubstituted morpholine to yield compounds 40 and 41 has been described previously.⁹

Determination of Cellular Potency and Dual PI3K and mTOR Kinase Activity. The structure–activity relationship (SAR) study focused initially on the exploration of substitutions on the morpholine moiety and its influence on PI3K versus mTOR inhibition. Therefore, two series of compounds were tested (Table 1): (i) symmetrical compounds (5 and 16–22), substituted with two identical morpholines (M_{1–7}) and (ii) asymmetric compounds (31–37), with one unsubstituted morpholine (M₀) and one substituted morpholine (M_{1–7}). Among the symmetric compounds, compound 20 (substituted with *cis*-3,5-dimethylmorpholine) had the highest affinity for both mTOR ($K_i = 40$ nM) and p110α ($K_i = 31$ nM). Overall, symmetric compounds with substituted morpholines showed increased concentrations for half-maximal inhibition (IC₅₀) of PKB/Akt and ribosomal protein S6 phosphorylation in cells. An exception was compound 17, substituted with (*S*)-3-methylmorpholine (M₂; IC₅₀ of 248 nM for pPKB and of 283 nM for pS6). With the exception of compound 31 (K_i for mTOR = 109 nM), asymmetric compounds showed a high in vitro potency for mTOR ($K_i < 65$ nM). Among this series, the most potent compounds toward PI3K and mTOR were 32 with one (*S*)-3-methylmorpholine (M₂) and 35 with *cis*-3,5-dimethylmorpholine (M₅; Table 1). The asymmetric compound 32 was 5-fold more potent on mTOR than its symmetric analogue bearing two (*S*)-3-methylmorpholine moieties (17) (K_i for mTOR = 25.5 and 137 nM, respectively). Overall, compounds with only

Table 2. SAR of Pyrimidine and Triazine Cores Substituted with Morpholine and (S)-3-Methylmorpholine



cpd.	X	Y	Z	W	cellular IC ₅₀ (nM) ^a		K _i (nM) ^b		K _i p110α/K _i mTOR	clog P ^c	PSA ^c
					pPKB	pS6	p110α	mTOR			
32	N	N	F	CH	195.7	89.8	8.3	25.5	0.33	3.52	102.52
6	N	N	H	CH	62.2	61.9	11.1	7.4	1.50	2.80	102.52
38	N	N	F	N	91.0	164	4.0	37.9	0.11	3.08	115.41
39	N	N	H	N	32.4	63.9	1.9	10.6	0.18	2.26	115.41
44	CH	N	H	CH	146	125	11.6	10.0	1.16	2.40	89.63
45	N	CH	H	CH	614	766	13.7	42.3	0.32	2.40	89.63
46	CH	N	H	N	77.3	146	4.1	15.3	0.27	1.85	102.52
47	N	CH	H	N	99.6	387	2.0	192	0.01	1.85	102.52

^aCellular phosphorylation of PKB/Akt on Ser473 and ribosomal S6 on Ser235/236 were analyzed in inhibitor-treated A2058 melanoma cells using in-cell western detection. Each experiment performed in triplicate or as a multiple of $n = 3$. ^bCompounds were tested in a time-resolved FRET (TR) assay (LanthaScreen), and inhibitor K_is were calculated for PI3Kα and mTOR, as described in Experimental Section. The PI3Kα/mTOR column depicts the ratio of compound-specific PI3Kα K_i over the K_i for mTOR. Each experiment was performed at least twice or as a multiple of $n = 2$. ^cMarvin/JChem 16.10.17 was used for calculation of logP (partition coefficient) and polar surface area (PSA) values.

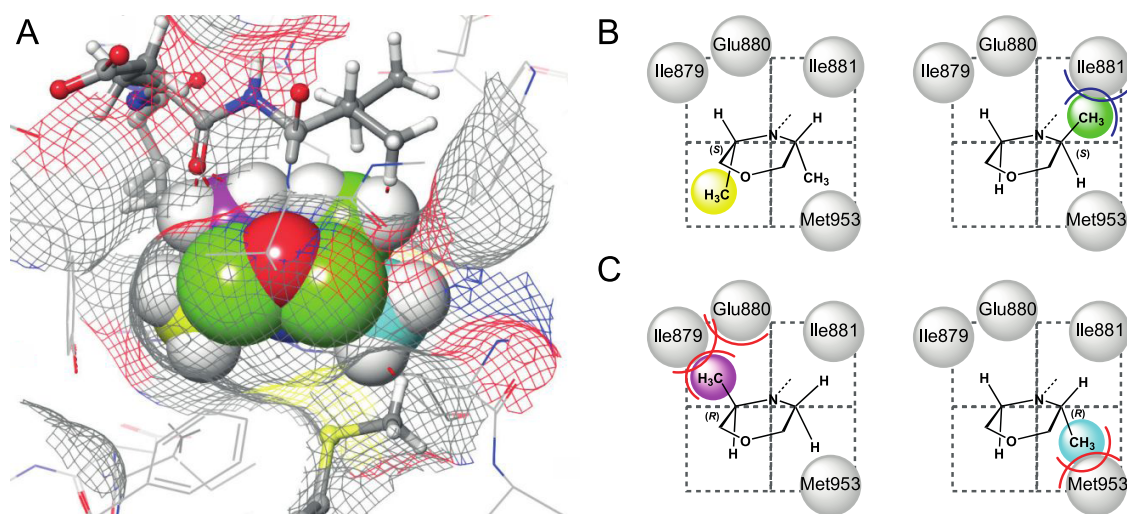


Figure 2. Model of PI3Kγ with docked compound **6** [(S)-enantiomer] and its (R)-enantiomer **66**. (A) The PI3Kγ surface is depicted as mesh, and selected amino acids are shown as sticks (gray). Two space-filling conformations of the methylmorpholino groups are shown for both **6** (green and yellow) and its enantiomer **66** (enantiomer, pink and cyan), oxygen atom pointing toward the hinge region Val882. The model is based on a PQR309 (S)-PI3Kγ complex (PDB ID: 5OQ4). Steric clashes conserved for class I PI3Ks are represented as red lines, and a steric clash detected PI3Kγ is indicated in blue. (B, C) Quadrant models for each possible position of the methyl substituent in the hinge region of PI3Kγ are depicted for (B) compound **6** and (C) compound **66**. In vitro PI3Kα binding affinities for **6** are 11.1 nM (K_i) and 20.8 nM (K_i) for **66** (see Table S2). For the p110α–compound **6** complex, see Figure S1 (deposited as PDB ID 6OAC).

one substituted morpholine were more potently inhibiting cellular PI3K/mTOR signaling. As compound **32** showed a 2-fold increase in affinity for both PI3K and mTOR with respect to PQR309 (S), it was selected for further optimization.

The results above, together with the SAR study that led to the development of a specific mTOR inhibitor, 5-[4,6-bis({3-oxa-8-azabicyclo[3.2.1]octan-8-yl})-1,3,5-triazin-2-yl]-4-(difluoromethyl)pyridin-2-amine (PQR620,^{17,18} **67**; for chemical structure, see Appendix S1 in the Supporting Information), encouraged the preparation of a compound series with (i) a (S)-3-methylmorpholine and (ii) a difluoro- or trifluoromethyl group on the heteroaryl moiety (Table 2). With the exception of compound **45**, both triazine (**6**, **32**, and **38–39**) and

pyrimidine (**44**, **46**, and **47**) core compounds showed very good potencies in cells. Moreover, these data confirmed our previous observation that 4-difluoromethyl-substituted heteroaryls yielded increased affinity for mTOR, compared to their respective 4-trifluoromethyl analogues.¹⁷ The introduction of an additional N-atom in the heteroaryl moiety moderately improved the affinity for PI3Kα (see K_i of 1.9 nM for **39** vs 11 nM for **6**; and K_i of 2.0 nM for **47** vs 14 nM for **45**), but reduced mTOR binding (K_i of 192 nM for **47** vs 42 nM for **45**), allowing a fine-tuning of PI3K/mTOR inhibition ratios. Although the pyrimidine core compound **44** showed a balanced PI3K/mTOR profile in vitro, compound **6** was selected (K_i for PI3Kα of ~11 nM and for mTOR of ~7.4 nM)

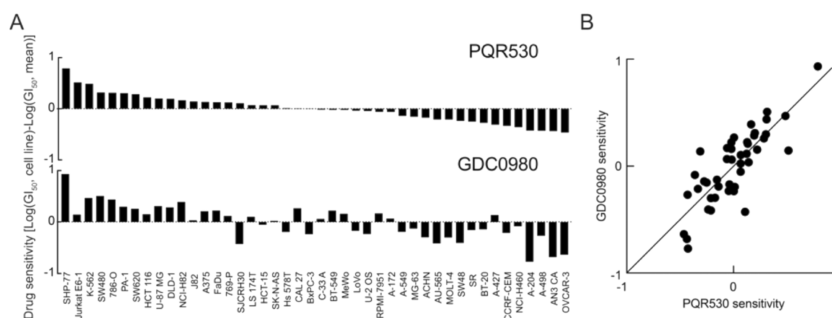


Figure 3. (A) Attenuation of cell proliferation in response to (S)-4-(difluoromethyl)-5-(4-(3-methylmorpholino)-6-morpholino-1,3,5-triazin-2-yl)pyridin-2-amine (PQR530) (**6**) and GDC0980 (**3**) represented as a waterfall plot. Concentrations of half-maximal growth inhibition (GI_{50}) were obtained from dose–response growth curves in 44 tumor cell lines. Log-transformed individual GI_{50} of a cell line was related to the log-transformed mean GI_{50} of all cell lines, and cell lines were sorted by lowest to highest sensitivity for PQR530 (**6**) from left to right. Individual cell lines and GI_{50} values are given in Table S5. (B) Correlation of **3** and **6** sensitivity of individual cell lines shown in (A). The comparative data set of **3** is from ref. 9. Further comparisons of cellular inhibition profiles for BEZ235 and compound **3** and **5** are shown in Figures S6 and S7.

for further characterization due to its superior activity in cells. Moreover, the triazine core yields symmetric compounds and, therefore, eases large-scale synthetic access.

Binding Mode to PI3K and mTOR. The binding mode and interactions of PQR309 (**5**)¹⁰ and BKM120 (**2**)⁹ with the ATP-binding site of PI3K γ have been elucidated. In detail, the orientation of the morpholine moiety in the hinge region is well understood and an identical binding mode for all class I PI3K isoforms can be assumed: the morpholine O atom forms a hydrogen-bond interaction with the hinge Val882 residue in PI3K γ (Val851 in PI3K α).

In 4-trifluoromethyl compounds with two equally substituted morpholines, morpholines **M**₁ (**16**), **M**₃ (**18**), **M**₄ (**19**), and **M**₇ (**22**) severely attenuated binding to PI3K α (Table 1; **M**₅ (**20**) and **M**₆ (**21**) had a minor effect, while **M**₂ (**17**) allowed to lower the K_i for p110 α to 7 nM). These results suggest that the (S)-enantiomer of methylmorpholine (**M**₂) is well accommodated when pointing toward the hinge region (PI3K γ : Val882; PI3K α : Val851), while the (**M**₁) substitution abrogates high-affinity interactions. Specifically, **17** with two (S)-methyl-morpholines (2 \times **M**₂) was 100-fold more potent on PI3K α than compound **16** with two (R)-methyl-morpholines (2 \times **M**₁; Table 1). This tendency was reproduced by compounds with a 4-difluoromethyl-substituted heteroaromatic group, where (S)-methylmorpholine substitutions (for example, 2 \times **M**₁ in **60**) augmented the affinity for PI3K α by 53-fold compared to **61** (with 2 \times **M**₂; see Table S2 in the Supporting Information). The orientation of the substituted morpholines toward the hinge Val was finally confirmed with a single-sided exchange of a substituted morpholine with piperidine—thus forcing the substituted morpholine to form a H-bond with the hinge Val (compounds **63**–**65** in Table S2).

To better understand the structural basis for the different affinity between compounds with (R)- and (S)-methyl-morpholines, computational modeling studies were carried out for compound **6** and its (R)-enantiomer (**66**): inhibitor–PI3K γ complexes were modeled using the PQR309 (**5**)/PI3K γ complex crystal structure (PDB ID: SOQ4) as a template to dock compounds with C3-substituted morpholines. As depicted in Figure 2, molecular modeling suggests a preferred placement of the (S)-methyl group pointing toward Tyr867 (Tyr836 in PI3K α), while a steric clash is flagged at Ile881. The (R)-methylmorpholine cannot be accommodated in PI3K γ , generating overlaps with the side chains of Ile879,

Glu880, and Met953. To validate this, a compound **6**–p110 α complex structure was resolved by X-ray crystallography at a resolution of 3.15 Å (PDB ID 6OAC; Figure S1). The core structure of compound **6** could be defined in the electron density, but distinct density for the methyl groups was not apparent (Figure S1). Fitting compound **6** to the obtained electron density map, the inhibitor was best accommodated with the methyl group in one of the two hydrophobic interfaces formed by side chains of Tyr836, Ile848, Ile932 or Trp780, Ile800, and Val850 (numbering referring to PI3K α). Val850 in PI3K α corresponds to Ile881 in PI3K γ , and the predicted steric clash at this position in PI3K γ could not be detected in PI3K α , which might explain in part a preferred binding of compound **6** to PI3K α versus PI3K γ (see Table S1; K_d for PI3K α = 0.84, K_d for PI3K γ = 10 nM). The lack of a distinct signal for the methyl group in the X-ray structure also suggests that compound **6** can bind to PI3Ks in multiple ways, with the substituted morpholine pointing toward either the hinge region (Figures 2 and S1) or the solvent exposed space.

A similar computational modeling analysis of the hinge region environment in mTOR showed that the ATP-binding pocket is wider: here, **M**₁ and **M**₂ [(R)- and (S)-methylmorpholine] can be accommodated (Figure S2). These findings are supported by comparison of compound **16** to **17** (Table 1), **59** to **61**, and **63** to **65** (Table S2), where mTOR affinities were very similar for **M**₁- and **M**₂-substituted compounds.

On- and Off-Target Activities. Compound **6** was selected for further elucidation of its activity profile. Binding of compound **6** to the ATP-binding site of PI3K α was confirmed by an in vitro Wortmannin¹⁹ competition assay, where **6** prevented covalent binding of wortmannin to Lys802 in PI3K α ²⁰ (Figure S3). The selectivity for PI3K and mTOR over a wide range of protein and lipid kinases was validated in a KINOMEScan panel. Here, the selectivity of compound **6** was compared to the data generated using the dual PI3K/mTOR inhibitor GDC0980 (**3**) and the structurally related pan-PI3K inhibitor **5**¹⁰ (Figure S4 and Table S4). Even at 10 μ M, compound **6** achieved excellent selectivity scores of $S(35)$ = 0.052 and $S(10)$ = 0.03, exceeding that of the dual PI3K/mTOR inhibitor **3** [$S(35)$ = 0.22, $S(10)$ = 0.09; for exact calculation, see Experimental Section; simplified: $S(35)$: fraction of total kinases with activities reduced to <35%].

Despite these differences in in vitro selectivity, the sensitivities of 44 tumor cell lines to **6** and **3** showed a good

overall correlation across the cell panel (Figure 3 and Table S5). Similarly, half-maximal growth inhibition (GI_{50}) of **6** (0.43 μ M in a 66 tumor cell line panel) was comparable to the mean GI_{50} of 44 cell lines **3** determined earlier (GI_{50} = 0.35 μ M).⁹ As observed before for other PI3K/mTOR inhibitors, compound **6** acted cytostatic, and minor cytotoxicity below 10 μ M was only observed in \sim 10% of cell lines at concentrations surpassing \gg 10 \times the GI_{50} (Table S5, individual growth curves are depicted in Figure S5).

Earlier reports have claimed that dual PI3K/mTOR inhibitors such as BEZ235^{5,6,21} outperform PI3K inhibitors in the suppression of cancer cell proliferation. However, these reports usually compared inhibitors that were structurally and pharmacologically very different. Indeed, the cell-specific sensitivity profile of 43 cell lines of BEZ235-mediated growth inhibition did not correlate significantly with the well-aligned profiles of **6** and **3** (Figure 3; for BEZ235, see Figure S6). A comparison of the impact of compound **6**, the structurally related PI3K inhibitor **5**, and the mTOR kinase inhibitor PQR620 (**67**) on cell proliferation and PI3K/mTOR signaling confirmed an increased potency of dual PI3K/mTOR inhibition by **6** compared to **5**, but was closely matched by **67** (Figure 4).

In line, compound **6** showed an increased potency in growth inhibition compared to **5** (average over 44 cell lines: 2.5- to 3-fold lower GI_{50} and IC_{50}). The very good correlation of the cellular inhibition profiles of **5** and **6** is compatible with a similar mode of action (Figure S7).

Interestingly, half-maximal growth inhibition is only achieved if phosphorylation of PKB/Akt is suppressed by ca. 90%. In SKOV3 cells, a constitutively activated p110 α mutant (H1047R) drives the PI3K/mTOR pathway, while A2058 cells are devoid of the phosphoinositide 3-phosphatase PTEN, and the B-Raf V600E mutation drives the activation of the mitogen-activated protein kinase pathway, which contributes to an increased resistance to PI3K and mTOR inhibitors. In both tumor cell lines, increased inhibition of mTOR by **6** enhanced its ability to suppress growth proliferation over that of **5**. While **67** demonstrated similar potency in these cells, in certain oncogenic contexts, a selective TORC1 inhibitor may not be desirable due to a loss of feedback inhibition (via S6K and IRS-1), resulting in reactivation of PI3K and PKB/Akt signaling (see ref 17 for a comparison of rapamycin and **67**). Thus, an inhibitor with high affinity toward both mTOR kinase and PI3K can be of advantage. The analysis of PI3K and mTOR downstream targets (PKB/Akt; GSK3 β , S6K, S6) confirmed that **6** has an enhanced potential to block the pathway compared to selective pan-PI3K or mTOR inhibitors.

Off-target effects of compound **6** were tested in a CEREP BioPrint (P22-p) panel at a concentration of 10 μ M. Only very weak competitions with radioligands for cell surface and nuclear receptors, membrane channels, transporters (Table S6) and enzyme activities of kinases, proteases, and phosphodiesterases (Table S7) were detected, suggesting that **6** is a safe compound.

Pharmacological Parameters. Metabolic stability of compound **6** was assessed in vitro prior to in vivo pharmacokinetic (PK) properties. When evaluated in human, rat, dog, and mouse liver microsomes, compound **6** showed little clearance (Cl) after 30 min of exposure (Table 3A). In hepatocyte cultures, compound **6** showed low clearance in all species, dog, rat, mouse, and human. The half-life of

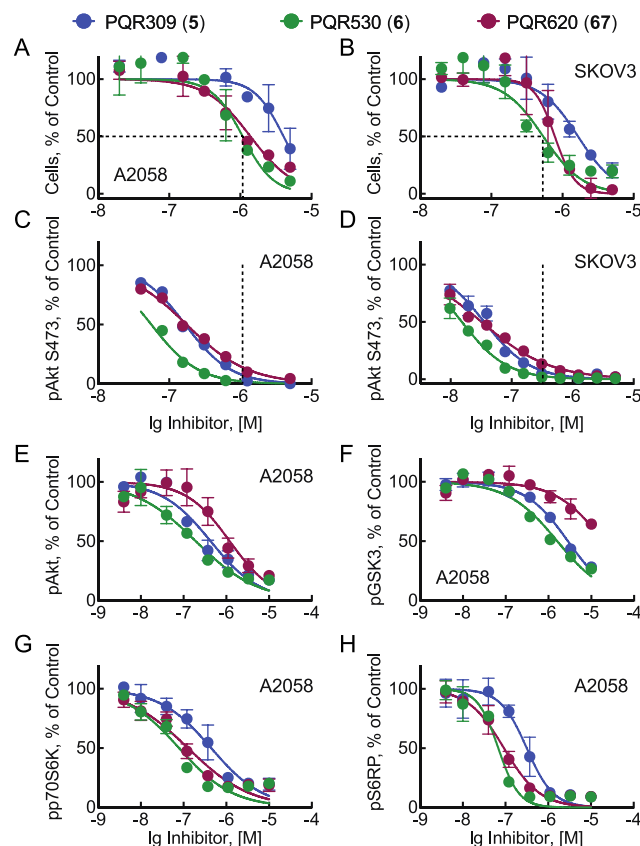


Figure 4. Impact of PI3K and mTOR inhibitors on cell proliferation and PI3K/mTOR downstream signaling. (A) A2058 and (B) SKOV3 cells were exposed to the indicated inhibitors for 72 h, and the resulting cell numbers are shown as % of dimethyl sulfoxide (DMSO) controls ($n = 2$, mean \pm standard deviation (SD)). The dotted lines connect 50% growth inhibition with phosphorylation of PKB/Akt on Ser473, analyzed in (C) A2058 and (D) SKOV3 cells after exposure to the indicated inhibitors for 1 h. Phosphoprotein levels were determined by an in-cell Western assay (mean \pm SD, $n = 3$). Phosphorylation of (E) PKB/Akt, (F) GSK3, (G) p70S6K, and (H) pS6 in A2058 lysates are shown as % of controls, detected using the Mesoscale Discovery platform (mean \pm SD, $n = 2$).

Table 3A. Stability in Liver Microsomes of Compound PQR530 (6**)**

cpd./species	% remaining in liver microsomes ^a			
	human	rat	dog	mouse
6	81.5	106	97.4	73.2
7-EC ^b	7.45	28.5	1.8	1.5
propranolol ^b	54.8	2.9	30.1	6.8

^aPercentage of compound remaining after 30 min (mean, $n = 2$).

^bAssay reference compounds: 7-EC, 7-ethoxycoumarin.

compound **6** was \sim 4.2 h in humans and, similarly, ca. 3.2–2.6 h in the other species (Table 3B).

Subsequently, PK parameters of compound **6** were assessed in male C57BL/6J mice using a single oral dose of 50 mg/kg (Table 4 and Figure 5). Drug levels were determined by liquid chromatography (LC)–tandem mass spectrometry in extracts of plasma, brain, and thigh muscle. Half-life was determined to be approximately 3.5–4.8 h. Concentration of compound **6** in the brain was higher than in plasma (C_{max} of \sim 7799 ng/mL in plasma and of \sim 12 627 ng/mL in brain), demonstrating that

Table 3B. Stability of Compound PQR530 (6) in Hepatocyte Cultures

cpd./species		human	rat	dog	mouse
6	CL _{int} ^a	6.0	7.0	10	11
	t _{1/2} (min)	250	192	142	142
7-EC ^b	CL _{int}	20.0	30	163.3	74
	t _{1/2} (min)	70.0	46.2	8.49	18.7
7-HC ^b	CL _{int}	65.5	124	138	116
	t _{1/2} (min)	21.1	11.1	10.2	11.9

^aCL_{int} (μL/(min 10⁶ cells)); t_{1/2} (min). ^bAssay reference compounds: 7-EC, 7-ethoxycoumarin; 7-HC, 7-hydroxycoumarin. Results are expressed as mean, n = 3.

Table 4. PK Analysis of PQR530 (6) after Oral Application in Male C57BL/6J Mice (50 mg/kg p.o.)^a

	plasma	brain	thigh muscle
C _{max} (ng/mL)	7799	12 627	11 946
T _{max} (h)	0.5	0.5	0.5
t _{1/2} (h)	4.7	4.8	3.5
AUC _{0–8h} (h ng/mL)	27 910	46 483	39 248
Cl (mL/(h kg))	1257	729	1003

^ap.o.: per os; C_{max}: maximal concentration; T_{max}: time of maximal concentration in hours; t_{1/2}: half-life elimination in hours; AUC: area under the curve; Cl: clearance; (n = 3, mean for each time point).

compound 6 passes the blood–brain barrier, showing an ~1:1.67 distribution between plasma and brain. The maximal concentration was reached after 30 min in plasma, brain, and thigh muscles.

The observed brain/plasma ratio corresponded with parallel artificial membrane permeability assay (PAMPA, Table S8A) and MDCK permeability assays, which documented a fast and passive diffusion. The lack of effect of the addition of the P-glycoprotein (P-gp) (P-glycoprotein 1, MDR1) inhibitor cyclosporine A to the MDCK assay demonstrates that 6 is not a substrate for P-gp transport (see Table S8B), which predicts excellent brain penetration. Finally, a brain tissue binding assay revealed a fu (fraction unbound) value of ~8%, which closely matched the levels of diazepam (fu ~ 9%, Table S8C) with a proven brain activity. Altogether, the assembled parameters characterize 6 as a compound with high on-target potency in brain tissue.

The physiological effect of compound 6 administration on plasma glucose and insulin levels in male C57BL/6J mice is shown in Figure 5: vehicle treatment did not affect plasma insulin or glucose levels, while compound 6 triggered an increase in plasma glucose and insulin levels. Ten minutes after treatment with compound 6, plasma glucose levels rose significantly compared to vehicle and reached maximal concentrations 1 h after dosing. Plasma insulin levels reached maxima 2 h post-dosing. The rise of plasma glucose and insulin levels are typical for PI3K/mTOR pathway inhibitors²² and have also been observed with pan-PI3K inhibitors, such as 5, in preclinical¹⁰ and phase I clinical studies.¹⁵

In vitro and in vivo toxicokinetic parameters were determined in rats and dogs, and are summarized in Table S9. The side effects of compound 6 were consistent with its mechanism of action. In Wistar rats, the no-observed adverse effect level (NOAEL) of compound 6 was considered to be 1 mg/(kg day) for males and 0.5 mg/kg for females

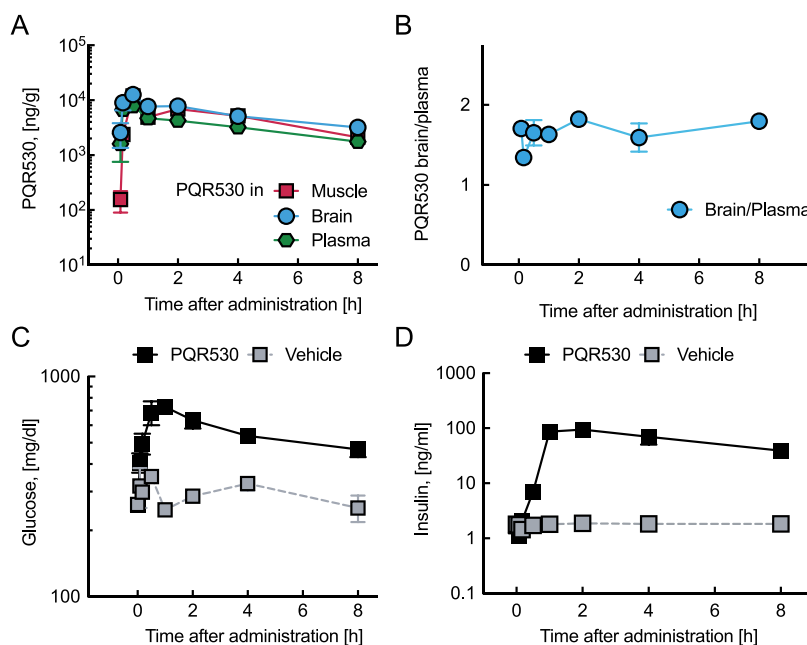


Figure 5. PK/pharmacodynamics (PD) assessment of PQR530 (6) in vivo. Compound 6 was administered to male C57BL/6J mice as single dose per os (p.o., 50 mg/kg). (A) Levels of 6 in C57BL/6J mouse tissues (muscle, brain, and plasma). Compound 6 was extracted from each tissue at the indicated time points and was subsequently quantified using LC–mass spectrometry (MS). (B) Tissue distribution ratios of 6. Data of 6 in (B) were compared to rapamycin and everolimus in ref 18. (C) Glucose concentration after oral application in male C57BL/6J mice. Plasma glucose was quantified using the Glucose Colorimetric Assay Kit (cat. No. Cay10009582-192, Biomol, Germany). (D) Plasma insulin levels in male C57BL/6J mice were quantified using a commercially available colorimetric immunoassay kit (Rat/Mouse Insulin ELISA, cat. No. EZRMI-13K, Merck Millipore, Germany). All values are mean ± standard error of the mean (SEM). Error bars are not shown when smaller than the symbols. A comparison of PK and brain/plasma distribution values of 6 with PQR309 (5) is shown in Figure S8.

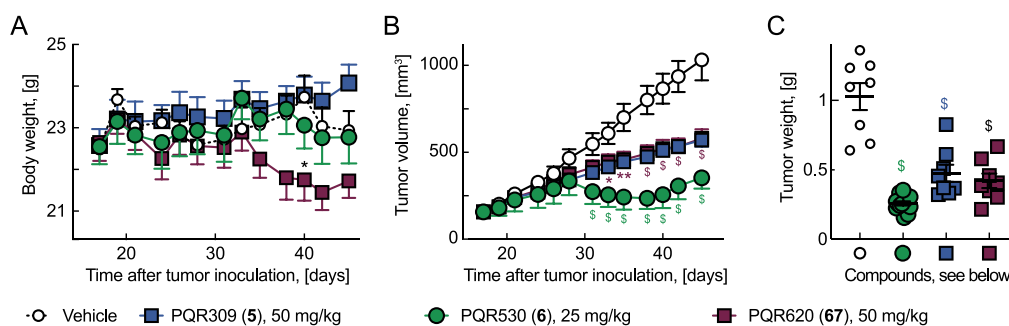


Figure 6. OVCAR-3 human ovarian cancer xenograft model in BALB/c nude mice: tumor cells were subcutaneously inoculated on day 0, and daily oral application of the indicated agents was started on day 17 (28 × QD). (A) Body weight was determined at the depicted time points. (B) The tumor size was measured and calculated as described in Experimental Section. (C) The tumor weight was determined on day 45. Statistics: * $p < 0.05$; ** $p < 0.001$; $^{\$}$ $p < 0.0001$; $n = 8$. (A, B) Two-way analysis of variance (ANOVA) with Bonferroni or Dunnett's correction for multicomplications; mean \pm SEM. (C) Mean \pm SEM; one-way ANOVA with Tukey's correction for multicomplications. PQR620 (67) and vehicle data were shown in ref 17.

(corresponding to steady-state AUC_{0-8} levels of 335 and 599 h ng/mL). In Beagle dogs, the no-observed adverse effect level (NOAEL) of compound 6 was 1 mg/(kg day) for males (corresponding to steady-state AUC_{last} levels of 127 ± 45 h ng/mL) and 3 mg/(kg day) for females (corresponding to steady-state AUC_{last} levels of 1070 ± 596 h ng/mL).

In Vivo Efficacy of PQR530 (6). To establish the antiproliferative effect of compound 6 in vivo, an OVCAR-3 xenograft model in BALB/c nude mice was used (Figure 6). To initiate tumor development, the mice were inoculated subcutaneously (region of right flank) with OVCAR-3 cells on day 0. From day 17, the control group received vehicle once a day (QD), while the treated group received 25 mg/kg of compound 6 p.o. QD. Compared to vehicle-treated mice, compound 6 significantly inhibited tumor growth. No significant body weight loss was observed.

CONCLUSIONS

An extensive SAR study led to the identification of 6, a potent ATP-competitive dual pan-PI3K and mTORC1/2 inhibitor with a subnanomolar K_d toward PI3K α and mTOR (0.84 and 0.33 nM, respectively). Compound 6 shows improved potency against mTOR kinase compared to other advanced candidates with dual pan class I PI3K and mTOR inhibitory activity. Molecular modeling and X-ray crystallography elucidated interactions of 6 in the ATP-binding pocket of PI3Ks and mTOR. The selectivity of 6 for PI3Ks and mTOR over a wide range of protein and lipid kinases, a lack of detectable off-target effects, and in vitro and in vivo toxicity studies highlight the safety of 6. Compound 6 displayed potency in inhibiting cancer cell line proliferation, and pharmacokinetic studies of 6 showed good bioavailability and excellent brain penetration, culminating in a good in vivo efficacy in an OVCAR-3 xenograft model. Altogether, the present results encourage the further development of the compound as a clinical candidate in oncology.

EXPERIMENTAL SECTION

General Information. Reagents were purchased at the highest commercial quality from Acros Organics, Sigma-Aldrich, or Fluorochem and used without further purification. Solvents were purchased from Acros Organics in AcroSeal bottles over molecular sieves. Cross-coupling reactions were carried out under nitrogen atmosphere in anhydrous solvents, and glassware was oven-dried prior to use. Thin-layer chromatography (TLC) plates were purchased

from Merck KGaA (Polygram SIL/UV254, 0.2 mm silica with fluorescence indicator), and UV light (254 nm) was used to visualize the compounds. Column chromatographic purifications were performed on Merck KGaA silica gel (pore size, 60 Å; 230–400 mesh particle size). Alternatively, flash chromatography was performed with Isco CombiFlash Companion systems using prepacked silica gel columns (40–60 μ m particle size RediSep). 1H , ^{19}F , and ^{13}C NMR spectra were recorded on a Bruker Avance 400 spectrometer. NMR spectra were obtained in deuterated solvents, such as $CDCl_3$ or $(CD_3)_2SO$. The chemical shifts (δ values) are reported in parts per million (ppm) and corrected to the signal of the deuterated solvents (7.26 ppm (1H NMR) and 77.16 ppm (^{13}C NMR) for $CDCl_3$, and 2.50 ppm (1H NMR) and 39.52 ppm (^{13}C NMR) for $(CD_3)_2SO$). ^{19}F NMR spectra are calibrated relative to $CFCl_3$ ($\delta = 0$ ppm) as external standard. When peak multiplicities are reported, the following abbreviations are used: s (singlet), d (doublet), dd (doublet of doublets), t (triplet), td (triplet of doublets), q (quartet), m (multiplet), br (broadened). Coupling constants, when given, are reported in hertz (Hz). High-resolution mass spectra were recorded on a Thermo Fisher Scientific LTQ Orbitrap XL (nano-electrospray ionization mass spectrometry) spectrometer. Matrix-assisted laser desorption ionization (MALDI) time-of-flight mass spectra were obtained on a Voyager-De Pro measured in m/z . The chromatographic purity of final compounds was determined by high-performance liquid chromatography (HPLC) analyses on an Ultimate 3000SD System from Thermo Fisher with LPG-3400SD pump system, ACC-3000 autosampler and column oven, and DAD-3000 diode array detector. An Acclaim-120 C18 reversed-phase column from Thermo Fisher was used as stationary phase. Gradient elution (5:95 for 0.2 min, 5:95 \rightarrow 100:0 over 10 min, 100:0 for 3 min) of the mobile phase consisting of $CH_3CN/MeOH:H_2O_{(10:90)}$ was used at a flow rate of 0.5 mL/min at 40 °C. The purity of all final compounds was higher than 95%.

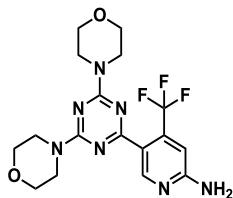
General Procedure 1. Step 1: Monochloro-triazine or -pyrimidine derivative (1.0 equiv), boronic acid pinacol ester 48 or 49 (1.0–1.1 equiv), K_3PO_4 (2.0–3.0 equiv), and chloro(2-dicyclohexylphosphino-2',4',6'-triisopropyl-1,1'-biphenyl)[2-(2'-amino-1,1'-biphenyl)]palladium(II) (XPhos Pd G2, 0.05 equiv) were charged in a flask. Under nitrogen atmosphere, absolute 1,4-dioxane (approx. 1 mL/0.2 mmol) and deionized H_2O (ca. 1 mL/0.4 mmol) were added and the resulting mixture was placed into an oil bath preheated at 95 °C and stirred at this temperature for 3–15 h. After completion of the reaction, the mixture was allowed to cool down to room temperature. Step 2: A 3 M aqueous HCl solution (>10 equiv) was added and the resulting mixture was heated at 60 °C for 3–15 h. Reaction completion was monitored by TLC. The mixture was allowed to cool down to room temperature, the pH was adjusted to 8–9 by addition of a 2 M aqueous NaOH solution and the aqueous layer was extracted with ethyl acetate (3 \times). The combined organic layers were dried over anhydrous Na_2SO_4 , filtered, and the solvent

was evaporated under reduced pressure. The crude product was purified by column chromatography on silica gel.

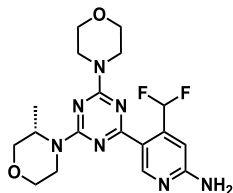
General Procedure 2. To a solution of 4-(4,6-dichloro-1,3,5-triazin-2-yl)morpholine (**23**, 1.0 equiv) in 1,4-dioxane (ca. 1 mL/0.3 mmol), the respective morpholine derivative (1.0–1.2 equiv) and *N,N*-diisopropylethylamine (4.5–4.7 equiv) were added. The resulting mixture was stirred at 70 °C overnight. The solvent was then removed under reduced pressure, and the residue was purified by column chromatography on silica gel.

General Procedure 3. Step 1: Bis(pinacolato)diboron (1.5 equiv), potassium acetate (3.0 equiv), [1,1'-bis(diphenylphosphino)ferrocene]dichloropalladium(II) (Pd(dppf)Cl₂, 0.10 equiv), and the respective bromo derivatives (1.0 equiv) were dissolved in absolute 1,4-dioxane (ca. 1 mL/0.2 mmol) under nitrogen atmosphere. The resulting mixture was heated at 95 °C for 6–8 h. Step 2: Then, the mixture was allowed to cool down to room temperature. Monochlorotriazine or -pyrimidine derivative (1.1 equiv), chloro(2-dicyclohexylphosphino-2',4',6'-triisopropyl-1,1'-biphenyl)[2-(2'-amino-1,1'-biphenyl)]palladium(II) (XPhos Pd G2, 0.05 equiv), K₃PO₄ (2.0 equiv), and deionized H₂O (ca. 1 mL/0.4 mmol) were added. The resulting reaction mixture was placed in a preheated oil bath at 95 °C and stirred for 3–15 h. After completion of the reaction, the mixture was allowed to cool down to room temperature, deionized H₂O was added, and the mixture was extracted with dichloromethane (3×). The combined organic layers were washed with brine (2×), dried over anhydrous Na₂SO₄, filtered, and reduced to dryness under reduced pressure. Step 3: The above residue was dissolved in 1,4-dioxane (ca. 1 mL/0.1 mmol) and an aqueous solution of HCl (3 M, 10–15 equiv) was added. The reaction mixture was stirred at 60 °C for 2 h. The mixture was diluted with deionized H₂O and washed with ethyl acetate (1×). The aqueous layer was basified to pH = 10 and then extracted with ethyl acetate (3×). The combined organic layers were dried over anhydrous Na₂SO₄, filtered, and reduced to dryness under reduced pressure. The crude product was purified by column chromatography on silica gel.

General Procedure 4. To a solution of the desired dichloropyrimidine (**40** or **41**, 1.0 equiv) in *N,N*-dimethylformamide (ca. 1 mL/0.3 mmol), the respective morpholine derivative (1.5 equiv) and *N,N*-diisopropylethylamine (3.0 equiv) were added. The resulting mixture was stirred at 130 °C overnight. The solvent was then removed under reduced pressure and the residue was dissolved in dichloromethane. The organic layer was washed with aqueous saturated NaHSO₄ solution, dried over anhydrous Na₂SO₄, filtered, and the solvent was evaporated under reduced pressure. The crude product was purified by column chromatography on silica gel.

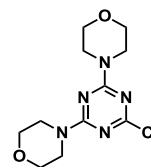


5-[4,6-bis(morpholin-4-yl)-1,3,5-triazin-2-yl]-4-(trifluoromethyl)pyridin-2-amine (PQR309, **5**). Compound **5** was prepared according to the literature.⁹

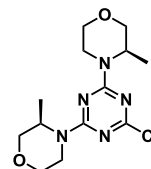


4-(Difluoromethyl)-5-{4-[(3S)-3-methylmorpholin-4-yl]-6-(morpholin-4-yl)-1,3,5-triazin-2-yl}pyridin-2-amine (PQR530, **6**). Pd(OAc)₂ (538 mg, 2.40 mmol, 0.04 equiv) and PPh₃ (1.89 g, 7.21 mmol, 0.12 equiv) were dissolved in tetrahydrofuran (50 mL) and stirred at room temperature for 1 h. This solution was added to a mixture of boronic acid pinacol ester **49** (19.5 g, 60.0 mmol, 1.0

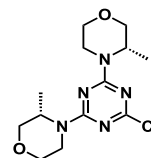
equiv), intermediate **25** (18.0 g, 60.0 mmol, 1.0 equiv), and aqueous K₂CO₃ (2.4 M, 81.0 mL, 194 mmol, 3.2 equiv) in tetrahydrofuran (200 mL). Then, the reaction mixture was heated at 55 °C for 2 h. After this time, the reaction mixture was allowed to cool down to room temperature and an aqueous HCl solution (5 M, 123 mL, 615 mmol, 10 equiv) was slowly added. The resulting reaction mixture was heated at 55 °C overnight. Upon completion of the reaction, the mixture was allowed to cool down to room temperature and tetrahydrofuran was removed under reduced pressure. The pH was adjusted to 9 by addition of NaOH pellets. The aqueous layer was extracted with 2-methyltetrahydrofuran (2 × 200 mL). The combined organic layers were dried over anhydrous Na₂SO₄, filtered, and concentrated to dryness under reduced pressure. The residue was purified by column chromatography on silica gel (cyclohexane/ethyl acetate 1:0 → 7:3) to afford compound **6** as a colorless solid (10.2 g, 25.0 mmol, 41%). ¹H NMR (400 MHz, CDCl₃): δ 9.03 (s, 1H), 7.67 (t, ¹J_{H,F} = 55 Hz, 1H), 6.84 (s, 1H), 4.84 (br s, 2H), 4.78–4.69 (m, 1H), 4.45–4.34 (m, 1H), 3.97 (dd, *J*_{H,H} = 11, 3.7 Hz, 1H), 3.89–3.71 (m, 9H), 3.68 (dd, *J*_{H,H} = 12, 3.2 Hz, 1H), 3.52 (td, *J*_{H,H} = 12, 3.0 Hz, 1H), 3.27 (td, *J*_{H,H} = 13, 3.8 Hz, 1H), 1.32 (d, ³J_{H,H} = 6.8 Hz, 3H). ¹⁹F{¹H} NMR (376 MHz, CDCl₃): δ -115.9 (s, 2F). ¹³C{¹H} NMR (101 MHz, CDCl₃): δ 169.4 (s, 1C), 164.9 (s, 1C), 164.5 (s, 1C), 160.2 (s, 1C), 152.5 (s, 1C), 143.7 (t, ²J_{C,F} = 22 Hz, 1C), 121.6 (t, ³J_{C,F} = 4.6 Hz, 1C), 111.5 (t, ¹J_{C,F} = 239 Hz, 1C), 104.1 (t, ³J_{C,F} = 7.9 Hz, 1C), 71.2 (s, 1C), 67.1 (s, 1C), 66.9 (br s, 2C), 46.5 (s, 1C), 43.8 (br s, 2C), 38.7 (s, 1C), 14.4 (s, 1C). Nanoelectrospray ionization-high-resolution mass spectrometry (NSI-HRMS) (*m/z*): [M + H]⁺ calcd for C₁₈H₂₄F₂N₇O₂, 408.1954; found: 408.1940. HPLC: *t*_R = 7.73 min (99.1% purity).



2-chloro-4,6-bis(morpholin-4-yl)-1,3,5-triazine (**8**). Compound **8** was prepared according to the literature.⁹

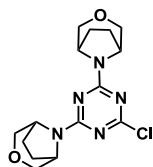


2-chloro-4,6-bis[(3R)-3-methylmorpholin-4-yl]-1,3,5-triazine (**9**). Compound **9** was prepared according to the literature.¹⁷

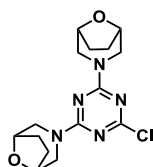


2-chloro-4,6-bis[(3S)-3-methylmorpholin-4-yl]-1,3,5-triazine (**10**). To a solution of cyanuric chloride (868 mg, 4.70 mmol, 1.0 equiv) in dichloromethane (20 mL) at 0 °C, a solution of (*S*)-3-methylmorpholine (2.00 g, 19.8 mmol, 4.2 equiv) in dichloromethane (20 mL) was slowly added. The resulting reaction mixture was stirred overnight, while it was allowed to warm up to room temperature. Additional dichloromethane (50 mL) was added and the organic layer was washed with an aqueous saturated NaHSO₄-solution (2×). The organic layer was dried over anhydrous Na₂SO₄, filtered, and the solvent was evaporated under reduced pressure. The crude product was purified by column chromatography on silica gel (cyclohexane/ethyl acetate 1:0 → 3:1) to afford compound **10** as a colorless solid (1.40 g, 4.46 mmol, 95%). ¹H NMR (400 MHz, CDCl₃): δ 4.76–4.53 (m, 2H), 4.39–4.22 (m, 2H), 3.93 (dd, *J*_{H,H} = 11, 3.7 Hz, 2H), 3.72 (d, *J*_{H,H} = 11 Hz, 2H), 3.63 (dd, *J*_{H,H} = 11, 3.2 Hz, 2H), 3.48 (td, *J*_{H,H} = 12, 3.0 Hz, 2H), 3.29–3.19 (m, 2H), 1.30 (d, ³J_{H,H} = 6.9 Hz, 6H).

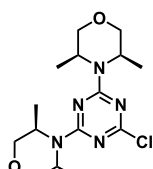
$^{13}\text{C}\{^1\text{H}\}$ NMR (101 MHz, CDCl_3): δ 169.7 (s, 1C), 164.3 (s, 2C), 71.0 (s, 2C), 67.0 (s, 2C), 46.8 (s, 2C), 38.9 (s, 2C), 14.6 (br s, 2C). MALDI-MS: $m/z = 314.4$ $[\text{M} + \text{H}]^+$.



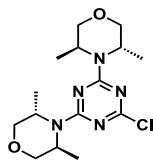
8-(4-Chloro-6-{3-oxa-8-azabicyclo[3.2.1]octan-8-yl}-1,3,5-triazin-2-yl)-3-oxa-8-azabicyclo[3.2.1]octane (**11**). Compound **11** was prepared according to the literature.⁹



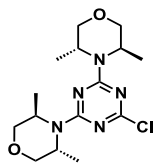
3-(4-Chloro-6-{8-oxa-3-azabicyclo[3.2.1]octan-3-yl}-1,3,5-triazin-2-yl)-8-oxa-3-azabicyclo[3.2.1]octane (**12**). Compound **12** was prepared according to the literature.¹⁷



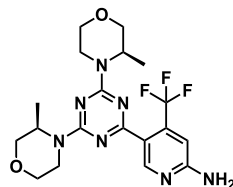
2-Chloro-4,6-bis[(3R,5S)-3,5-dimethylmorpholin-4-yl]-1,3,5-triazine (**13**). Compound **13** was prepared according to the literature.¹⁷



2-Chloro-4,6-bis[(3S,5S)-3,5-dimethylmorpholin-4-yl]-1,3,5-triazine (**14**). Compound **14** was prepared according to the literature.¹⁷

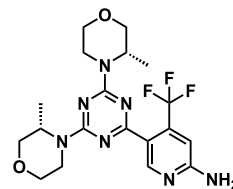


2-Chloro-4,6-bis[(3R,5R)-3,5-dimethylmorpholin-4-yl]-1,3,5-triazine (**15**). Compound **15** was prepared according to the literature.¹⁷

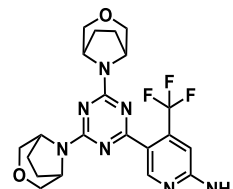


5-[4,6-Bis[(3R)-3-methylmorpholin-4-yl]-1,3,5-triazin-2-yl]-4-(trifluoromethyl)pyridin-2-amine (**16**). Compound **16** was prepared according to general procedure 1 from intermediate **9** (80.0 mg, 255 μmol , 1.0 equiv) and boronic acid pinacol ester **48** (87.1 mg, 254 μmol , 1.0 equiv). Purification by column chromatography on silica gel (cyclohexane/ethyl acetate 1:0 \rightarrow 4:6) gave compound **16** as a colorless solid (71.0 mg, 162 μmol , 64%). ^1H NMR (400 MHz, CDCl_3): δ 8.72 (s, 1H), 6.78 (s, 1H), 4.91 (br s, 2H), 4.85–4.70 (m, 2H), 4.51–4.33 (m, 2H), 3.95 (dd, $^2J_{\text{H,H}} = 11$ Hz, $^3J_{\text{H,H}} = 3.6$ Hz, 2H), 3.74 (d, $^2J_{\text{H,H}} = 11$ Hz, 2H), 3.66 (dd, $^2J_{\text{H,H}} = 11$ Hz, $^3J_{\text{H,H}} = 3.2$ Hz, 2H), 3.51 (td, $J_{\text{H,H}} = 12$, 3.0 Hz, 2H), 3.31–3.19 (m, 2H), 1.32 (d, $^3J_{\text{H,H}} = 6.8$ Hz, 6H). $^{19}\text{F}\{^1\text{H}\}$ NMR (376 MHz, CDCl_3): δ -60.2 (s, 3F). $^{13}\text{C}\{^1\text{H}\}$ NMR (101 MHz, CDCl_3): δ 169.9 (s, 1C), 164.5 (s, 2C), 159.6 (s, 1C), 152.9 (s, 1C), 138.5 (q, $^2J_{\text{C,F}} = 33$ Hz, 1C), 123.0

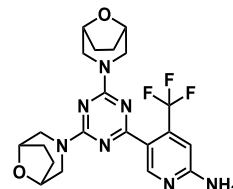
(q, $^1J_{\text{C,F}} = 274$ Hz, 1C), 122.6 (s, 1C), 105.7–105.2 (s, 1C), 71.2 (s, 2C), 67.2 (s, 2C), 46.4 (s, 2C), 38.6 (s, 2C), 14.4 (s, 2C). NSI-HRMS (m/z): $[\text{M} + \text{H}]^+$ calcd for $\text{C}_{19}\text{H}_{25}\text{F}_3\text{N}_7\text{O}_2$, 440.2016; found: 440.2007. HPLC: $t_{\text{R}} = 8.50$ min (98.1% purity).



5-[4,6-Bis[(3S)-3-methylmorpholin-4-yl]-1,3,5-triazin-2-yl]-4-(trifluoromethyl)pyridin-2-amine (**17**). Compound **17** was prepared according to general procedure 1 from intermediate **10** (700 mg, 2.23 mmol, 1.0 equiv) and boronic acid pinacol ester **48** (770 mg, 2.24 mmol, 1.0 equiv). Purification by column chromatography on silica gel (cyclohexane/ethyl acetate 1:2 \rightarrow 1:3) gave compound **17** as a colorless solid (344 mg, 782 μmol , 35%). ^1H NMR (400 MHz, CDCl_3): δ 8.70 (s, 1H), 6.76 (s, 1H), 4.84 (br s, 2H), 4.81–4.69 (m, 2H), 4.48–4.30 (m, 2H), 3.93 (dd, $^2J_{\text{H,H}} = 11$ Hz, $^3J_{\text{H,H}} = 3.7$ Hz, 2H), 3.73 (d, $^2J_{\text{H,H}} = 11$ Hz, 2H), 3.64 (dd, $^3J_{\text{H,H}} = 12$ Hz, $^2J_{\text{H,H}} = 3.2$ Hz, 2H), 3.55–3.45 (m, 2H), 3.28–3.18 (m, 2H), 1.30 (d, $^3J_{\text{H,H}} = 6.8$ Hz, 6H). $^{19}\text{F}\{^1\text{H}\}$ NMR (376 MHz, CDCl_3): δ -60.2 (s, 3F). $^{13}\text{C}\{^1\text{H}\}$ NMR (101 MHz, CDCl_3): δ 169.9 (s, 1C), 164.5 (s, 2C), 159.6 (s, 1C), 152.8 (s, 1C), 138.5 (q, $^2J_{\text{C,F}} = 33$ Hz, 1C), 123.0 (q, $^1J_{\text{C,F}} = 274$ Hz, 1C), 122.5 (s, 1C), 105.7–105.1 (s, 1C), 71.2 (s, 2C), 67.1 (s, 2C), 46.4 (s, 2C), 38.5 (s, 2C), 14.4 (s, 2C). NSI-HRMS (m/z): $[\text{M} + \text{H}]^+$ calcd for $\text{C}_{19}\text{H}_{25}\text{F}_3\text{N}_7\text{O}_2$, 440.2016; found: 440.2006. HPLC: $t_{\text{R}} = 8.49$ min (99.0% purity).

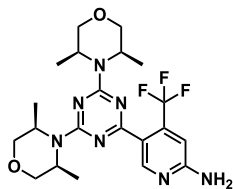


5-[4,6-Bis[(3-oxa-8-azabicyclo[3.2.1]octan-8-yl)-1,3,5-triazin-2-yl]-4-(trifluoromethyl)pyridin-2-amine (**18**). Compound **18** was prepared according to general procedure 1 from intermediate **11** (100 mg, 296 μmol , 1.0 equiv) and boronic acid pinacol ester **48** (112 mg, 325 μmol , 1.1 equiv). Purification by column chromatography on silica gel (cyclohexane/ethyl acetate 1:0 \rightarrow 3:7) gave compound **18** as a colorless solid (118 mg, 255 μmol , 87%). ^1H NMR (400 MHz, CDCl_3): δ 8.71 (s, 1H), 6.77 (s, 1H), 4.90 (br s, 2H), 4.80–4.59 (m, 4H), 3.83–3.73 (m, 4H), 3.67–3.58 (m, 4H), 2.13–1.92 (m, 8H). $^{19}\text{F}\{^1\text{H}\}$ NMR (376 MHz, CDCl_3): δ -59.9 (s, 3F). $^{13}\text{C}\{^1\text{H}\}$ NMR (101 MHz, CDCl_3): δ 170.4 (s, 1C), 163.4 (s, 2C), 159.6 (s, 1C), 152.8 (s, 1C), 138.5 (q, $^2J_{\text{C,F}} = 33$ Hz, 1C), 123.0 (q, $^1J_{\text{C,F}} = 274$ Hz, 1C), 122.5 (s, 1C), 105.5 (q, $^3J_{\text{C,F}} = 6.0$ Hz, 1C), 72.1 (s, 2C), 71.7 (s, 2C), 54.9 (s, 2C), 54.5 (s, 2C), 27.0 (s, 4C). NSI-HRMS (m/z): $[\text{M} + \text{H}]^+$ calcd for $\text{C}_{21}\text{H}_{25}\text{F}_3\text{N}_7\text{O}_2$, 464.2016; found: 464.1999. HPLC: $t_{\text{R}} = 8.33$ min (97.1% purity).

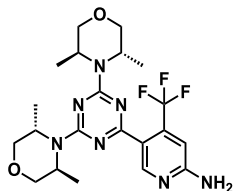


5-[4,6-Bis[(8-oxa-3-azabicyclo[3.2.1]octan-3-yl)-1,3,5-triazin-2-yl]-4-(trifluoromethyl)pyridin-2-amine (**19**). Compound **19** was prepared according to general procedure 1 from intermediate **12** (100 mg, 296 μmol , 1.0 equiv) and boronic acid pinacol ester **48** (112 mg, 325 μmol , 1.1 equiv). Purification by column chromatography on silica gel (cyclohexane/ethyl acetate 1:0 \rightarrow 3:7) gave compound **19** as a colorless solid (105 mg, 227 μmol , 77%). ^1H NMR (400 MHz, CDCl_3): δ 8.69 (s, 1H), 6.77 (s, 1H), 4.89 (br s, 2H), 4.48–4.37 (m,

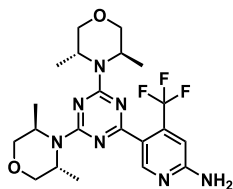
6H), 4.35–4.25 (m, 2H), 3.21–3.12 (m, 4H), 1.97–1.87 (m, 4H), 1.83–1.73 (m, 4H). $^{19}\text{F}\{^1\text{H}\}$ NMR (376 MHz, CDCl_3): δ -59.8 (s, 3F). $^{13}\text{C}\{^1\text{H}\}$ NMR (101 MHz, CDCl_3): δ 169.6 (s, 1C), 165.7 (s, 2C), 159.6 (s, 1C), 152.8 (s, 1C), 138.5 (q, $^2J_{\text{C,F}} = 33$ Hz, 1C), 123.0 (q, $^1J_{\text{C,F}} = 274$ Hz, 1C), 122.7 (s, 1C), 105.4 (q, $^3J_{\text{C,F}} = 5.7$ Hz, 1C), 74.2 (s, 2C), 74.0 (s, 2C), 49.4 (s, 2C), 49.1 (s, 2C), 27.9 (s, 2C), 27.7 (s, 2C). NSI-HRMS (m/z): $[\text{M} + \text{H}]^+$ calcd for $\text{C}_{21}\text{H}_{25}\text{F}_3\text{N}_7\text{O}_2$, 464.2016; found: 464.1998. HPLC: $t_{\text{R}} = 8.07$ min (97.1% purity).



5-[4,6-Bis((3R,5S)-3,5-dimethylmorpholin-4-yl)-1,3,5-triazin-2-yl]-4-(trifluoromethyl)pyridin-2-amine (20). Compound 20 was prepared according to general procedure 1 from intermediate 13 (48.0 mg, 140 μmol , 1.0 equiv) and boronic acid pinacol ester 48 (53.0 mg, 154 μmol , 1.1 equiv). Purification by column chromatography on silica gel (cyclohexane/ethyl acetate 1:0 \rightarrow 1:1) gave compound 20 as a colorless solid (29.3 mg, 62.7 μmol , 44%). ^1H NMR (400 MHz, CDCl_3): δ 8.78 (s, 1H), 6.79 (s, 1H), 4.82 (br s, 2H), 4.71–4.50 (m, 4H), 3.82 (d, $^2J_{\text{H,H}} = 11$ Hz, 4H), 3.64 (dd, $^2J_{\text{H,H}} = 11$ Hz, $^3J_{\text{H,H}} = 3.4$ Hz, 4H), 1.37 (d, $^3J_{\text{H,H}} = 6.9$ Hz, 12H). $^{19}\text{F}\{^1\text{H}\}$ NMR (376 MHz, CDCl_3): δ -60.4 (s, 3F). $^{13}\text{C}\{^1\text{H}\}$ NMR (101 MHz, CDCl_3): δ 169.6 (s, 1C), 164.2 (s, 2C), 159.4 (s, 1C), 153.1 (s, 1C), 138.5 (q, $^2J_{\text{C,F}} = 33$ Hz, 1C), 123.0 (q, $^1J_{\text{C,F}} = 274$ Hz, 1C), 122.9 (s, 1C), 105.4 (q, $^3J_{\text{C,F}} = 5.7$ Hz, 1C), 71.6 (s, 4C), 45.7 (s, 4C), 19.3 (br s, 4C). NSI-HRMS (m/z): $[\text{M} + \text{H}]^+$ calcd for $\text{C}_{21}\text{H}_{29}\text{F}_3\text{N}_7\text{O}_2$, 468.2329; found: 468.2311. HPLC: $t_{\text{R}} = 9.72$ min (97.2% purity).

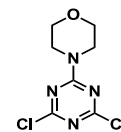


5-[4,6-Bis((3S,5S)-3,5-dimethylmorpholin-4-yl)-1,3,5-triazin-2-yl]-4-(trifluoromethyl)pyridin-2-amine (21). Compound 21 was prepared according to general procedure 1 from intermediate 14 (185 mg, 541 μmol , 1.0 equiv) and boronic acid pinacol ester 48 (205 mg, 597 μmol , 1.1 equiv). Purification by column chromatography on silica gel (cyclohexane/ethyl acetate 1:0 \rightarrow 7:3) gave compound 21 as a colorless solid (143 mg, 306 μmol , 57%). ^1H NMR (400 MHz, CDCl_3): δ 8.77 (s, 1H), 6.79 (s, 1H), 4.82 (br s, 2H), 4.45–4.34 (m, 4H), 4.23 (dd, $^2J_{\text{H,H}} = 11$ Hz, $^3J_{\text{H,H}} = 3.3$ Hz, 4H), 3.74 (dd, $^2J_{\text{H,H}} = 11$ Hz, $^3J_{\text{H,H}} = 2.3$ Hz, 4H), 1.46 (d, $^3J_{\text{H,H}} = 6.6$ Hz, 12H). $^{19}\text{F}\{^1\text{H}\}$ NMR (376 MHz, CDCl_3): δ -60.4 (s, 3F). $^{13}\text{C}\{^1\text{H}\}$ NMR (101 MHz, CDCl_3): δ 169.4 (s, 1C), 164.1 (s, 2C), 159.4 (s, 1C), 153.1 (s, 1C), 138.3 (q, $^2J_{\text{C,F}} = 33$ Hz, 1C), 123.0 (q, $^1J_{\text{C,F}} = 274$ Hz, 1C), 122.8 (s, 1C), 105.5–105.1 (m, 1C), 68.0 (s, 4C), 48.0 (s, 4C), 19.8 (s, 4C). NSI-HRMS (m/z): $[\text{M} + \text{H}]^+$ calcd for $\text{C}_{21}\text{H}_{29}\text{F}_3\text{N}_7\text{O}_2$, 468.2329; found: 468.2321. HPLC: $t_{\text{R}} = 9.30$ min (98.6% purity).

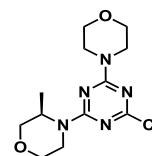


5-[4,6-Bis((3R,5R)-3,5-dimethylmorpholin-4-yl)-1,3,5-triazin-2-yl]-4-(trifluoromethyl)pyridin-2-amine (22). Compound 22 was prepared according to general procedure 1 from intermediate 15 (229 mg, 670 μmol , 1.0 equiv) and boronic acid pinacol ester 48 (250 mg, 729 μmol , 1.1 equiv). Purification by column chromatography on silica gel (cyclohexane/ethyl acetate 1:0 \rightarrow 6:4) gave compound 22 as a yellowish solid (110 mg, 235 μmol , 35%). ^1H NMR (400 MHz,

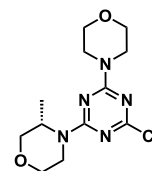
CDCl_3): δ 8.77 (s, 1H), 6.79 (s, 1H), 4.83 (br s, 2H), 4.46–4.34 (m, 4H), 4.23 (dd, $^2J_{\text{H,H}} = 11$ Hz, $^3J_{\text{H,H}} = 3.3$ Hz, 4H), 3.74 (dd, $^2J_{\text{H,H}} = 11$ Hz, $^3J_{\text{H,H}} = 2.2$ Hz, 4H), 1.45 (d, $^3J_{\text{H,H}} = 6.6$ Hz, 12H). $^{19}\text{F}\{^1\text{H}\}$ NMR (376 MHz, CDCl_3): δ -60.4 (s, 3F). $^{13}\text{C}\{^1\text{H}\}$ NMR (101 MHz, CDCl_3): δ 169.4 (s, 1C), 164.1 (s, 2C), 159.4 (s, 1C), 153.1 (s, 1C), 138.3 (q, $^2J_{\text{C,F}} = 33$ Hz, 1C), 123.0 (q, $^1J_{\text{C,F}} = 274$ Hz, 1C), 122.8 (s, 1C), 105.5–105.0 (m, 1C), 68.0 (s, 4C), 48.0 (s, 4C), 19.8 (s, 4C). NSI-HRMS (m/z): $[\text{M} + \text{H}]^+$ calcd for $\text{C}_{21}\text{H}_{29}\text{F}_3\text{N}_7\text{O}_2$, 468.2329; found: 468.2313. HPLC: $t_{\text{R}} = 9.31$ min (96.2% purity).



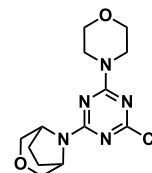
2,4-Dichloro-6-(morpholin-4-yl)-1,3,5-triazine (23). Compound 23 was prepared according to the literature.⁹



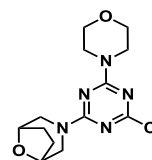
2-Chloro-4-[(3R)-3-methylmorpholin-4-yl]-6-(morpholin-4-yl)-1,3,5-triazine (24). Compound 24 was prepared according to the literature.¹⁷



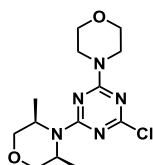
2-Chloro-4-[(3S)-3-methylmorpholin-4-yl]-6-(morpholin-4-yl)-1,3,5-triazine (25). To a solution of (S)-3-methylmorpholine (560 mg, 5.54 mmol, 1.2 equiv) and *N,N*-diisopropylethylamine (1.70 mL, 9.76 mmol, 2.1 equiv) in ethanol (10 mL) at 0 $^\circ\text{C}$, 4-(4,6-dichloro-1,3,5-triazin-2-yl)morpholine (23, 1.11 g, 4.72 mmol, 1.0 equiv) was added portionwise. The resulting mixture was stirred at room temperature overnight. The solvent was removed under reduced pressure and the residue was purified by column chromatography on silica gel (cyclohexane/ethyl acetate 1:0 \rightarrow 4:1) to afford compound 25 as a colorless solid (1.46 g, 4.87 mmol, 74%). ^1H NMR (400 MHz, CDCl_3): δ 4.75–4.57 (m, 1H), 4.40–4.23 (m, 1H), 3.93 (dd, $J_{\text{H,H}} = 11$, 3.8 Hz, 1H), 3.85–3.67 (m, 9H), 3.63 (dd, $J_{\text{H,H}} = 11$, 3.2 Hz, 1H), 3.48 (td, $J_{\text{H,H}} = 12$, 2.9 Hz, 1H), 3.29–3.20 (m, 1H), 1.30 (d, $^3J_{\text{H,H}} = 6.9$ Hz, 3H). $^{13}\text{C}\{^1\text{H}\}$ NMR (101 MHz, CDCl_3): δ 169.8 (s, 1C), 164.6 (s, 1C), 164.3 (s, 1C), 71.0 (s, 1C), 66.9 (s, 1C), 66.7 (br s, 2C), 46.8 (s, 1C), 43.9 (s, 2C), 38.9 (s, 1C), 14.5 (br s, 1C). MALDI-MS: $m/z = 300.3$ $[\text{M} + \text{H}]^+$.



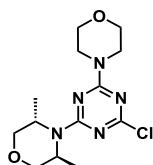
8-[4-Chloro-6-(morpholin-4-yl)-1,3,5-triazin-2-yl]-3-oxa-8-azabicyclo[3.2.1]octane (26). Compound 26 was prepared according to the literature.¹⁷



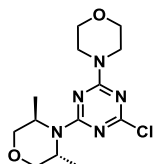
3-[4-Chloro-6-(morpholin-4-yl)-1,3,5-triazin-2-yl]-8-oxa-3-azabicyclo[3.2.1]octane (27). Compound 27 was prepared according to the literature.¹⁷



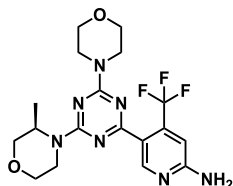
2-Chloro-4-[(3R,5S)-3,5-dimethylmorpholin-4-yl]-6-(morpholin-4-yl)-1,3,5-triazine (28). Compound **28** was prepared according to general procedure 2 from (3R,5S)-3,5-dimethylmorpholine (160 mg, 1.39 mmol, 1.1 equiv) and 4-(4,6-dichloro-1,3,5-triazin-2-yl)morpholine (**23**, 304 mg, 1.29 mmol, 1.0 equiv) in the presence of *N,N*-diisopropylethylamine (1.05 mL, 6.03 mmol, 4.7 equiv). Purification by column chromatography on silica gel (cyclohexane/ethyl acetate 1:0 → 4:1) gave compound **28** as a colorless solid (297 mg, 1.39 mmol, 73%). ¹H NMR (400 MHz, CDCl₃): δ 4.55–4.43 (m, 2H), 3.81–3.73 (m, 6H), 3.71–3.67 (m, 4H), 3.59 (dd, ²J_{H,H} = 12 Hz, ³J_{H,H} = 3.9 Hz, 2H), 1.34 (d, ³J_{H,H} = 7.0 Hz, 6H). ¹³C{¹H} NMR (101 MHz, CDCl₃): δ 169.7 (s, 1C), 164.6 (s, 1C), 164.1 (s, 1C), 71.3 (s, 2C), 66.7 (br s, 2C), 46.2 (s, 2C), 43.9 (s, 2C), 19.1 (br s, 2C). MALDI-MS: *m/z* = 314.2 [M + H]⁺.



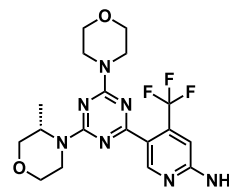
2-Chloro-4-[(3S,5S)-3,5-dimethylmorpholin-4-yl]-6-(morpholin-4-yl)-1,3,5-triazine (29). Compound **29** was prepared according to general procedure 2 from (3S,5S)-3,5-dimethylmorpholine (182 mg, 1.58 mmol, 1.2 equiv) and 4-(4,6-dichloro-1,3,5-triazin-2-yl)morpholine (**23**, 304 mg, 1.29 mmol, 1.0 equiv) in the presence of *N,N*-diisopropylethylamine (1.00 mL, 5.74 mmol, 4.5 equiv). Purification by column chromatography on silica gel (cyclohexane/ethyl acetate 1:0 → 4:1) gave compound **29** as a colorless solid (351 mg, 1.12 mmol, 87%). ¹H NMR (400 MHz, CDCl₃): δ 4.35–4.26 (m, 2H), 4.19 (dd, ²J_{H,H} = 11 Hz, ³J_{H,H} = 3.3 Hz, 2H), 3.85–3.68 (m, 8H), 1.41 (d, ³J_{H,H} = 6.7 Hz, 6H). ¹³C{¹H} NMR (101 MHz, CDCl₃): δ 169.4 (s, 1C), 164.5 (s, 1C), 164.2 (s, 1C), 67.6 (s, 2C), 66.8 (br s, 2C), 48.4 (s, 2C), 44.0 (s, 2C), 19.6 (s, 2C). MALDI-MS: *m/z* = 314.2 [M + H]⁺.



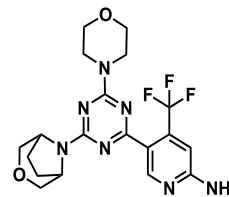
2-Chloro-4-[(3R,5R)-3,5-dimethylmorpholin-4-yl]-6-(morpholin-4-yl)-1,3,5-triazine (30). Compound **30** was prepared according to general procedure 2 from (3R,5R)-3,5-dimethylmorpholine (250 mg, 2.17 mmol, 1.2 equiv) and 4-(4,6-dichloro-1,3,5-triazin-2-yl)morpholine (**23**, 434 mg, 1.85 mmol, 1.0 equiv) in the presence of *N,N*-diisopropylethylamine (1.50 mL, 8.61 mmol, 4.7 equiv). Purification by column chromatography on silica gel (cyclohexane/ethyl acetate 1:0 → 4:1) gave compound **30** as a colorless solid (504 mg, 1.61 mmol, 87%). ¹H NMR (400 MHz, CDCl₃): δ 4.35–4.25 (m, 2H), 4.17 (dd, ²J_{H,H} = 11 Hz, ³J_{H,H} = 3.3 Hz, 2H), 3.84–3.64 (m, 10H), 1.40 (d, ³J_{H,H} = 6.7 Hz, 6H). ¹³C{¹H} NMR (101 MHz, CDCl₃): δ 169.4 (s, 1C), 164.4 (s, 1C), 164.1 (s, 1C), 67.5 (s, 2C), 66.7 (br s, 2C), 48.4 (s, 2C), 43.9 (br s, 2C), 19.5 (br s, 2C). MALDI-MS: *m/z* = 314.3 [M + H]⁺.



5-[4-[(3R)-3-Methylmorpholin-4-yl]-6-(morpholin-4-yl)-1,3,5-triazin-2-yl]-4-(trifluoromethyl)pyridin-2-amine (31). Compound **31** was prepared according to general procedure 1 from intermediate **24** (100 mg, 334 μmol, 1.0 equiv) and boronic acid pinacol ester **48** (130 mg, 379 μmol, 1.1 equiv). Purification by column chromatography on silica gel (cyclohexane/ethyl acetate 1:0 → 3:7) gave compound **31** as a colorless solid (45.5 mg, 107 μmol, 32%). ¹H NMR (400 MHz, CDCl₃): δ 8.72 (s, 1H), 6.79 (s, 1H), 4.92–4.71 (m, 3H), 4.52–4.32 (m, 1H), 4.04–3.91 (m, 1H), 3.91–3.79 (m, 4H), 3.77–3.63 (m, 6H), 3.57–3.46 (m, 1H), 3.32–3.20 (m, 1H), 1.32 (d, ³J_{H,H} = 6.8 Hz, 3H). ¹⁹F{¹H} NMR (376 MHz, CDCl₃): δ -60.2 (s, 3F). ¹³C{¹H} NMR (101 MHz, CDCl₃): δ 170.0 (s, 1C), 164.9 (s, 1C), 164.5 (s, 1C), 159.6 (s, 1C), 152.8 (s, 1C), 138.5 (q, ²J_{C,F} = 33 Hz, 1C), 123.0 (q, ¹J_{C,F} = 274 Hz, 1C), 122.5 (br s, 1C), 105.5 (q, ³J_{C,F} = 6.1 Hz, 1C), 71.2 (s, 1C), 67.2 (s, 1C), 66.9 (br s, 2C), 46.4 (s, 1C), 43.7 (br s, 2C), 38.6 (s, 1C), 14.4 (s, 1C). NSI-HRMS (*m/z*): [M + H]⁺ calcd for C₁₈H₂₃F₃N₇O₂, 426.1860; found: 426.1856. HPLC: *t_R* = 7.96 min (96.4% purity).

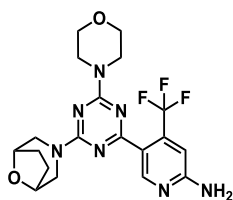


5-[4-[(3S)-3-Methylmorpholin-4-yl]-6-(morpholin-4-yl)-1,3,5-triazin-2-yl]-4-(trifluoromethyl)pyridin-2-amine (32). Compound **32** was prepared according to general procedure 1 from intermediate **25** (80.0 mg, 268 μmol, 1.0 equiv) and boronic acid pinacol ester **48** (94.0 mg, 273 μmol, 1.0 equiv). Purification by column chromatography on silica gel (cyclohexane/ethyl acetate 1:0 → 3:7) gave compound **32** as a colorless solid (84.1 mg, 198 μmol, 74%). ¹H NMR (400 MHz, CDCl₃): δ 8.72 (s, 1H), 6.79 (s, 1H), 4.90–4.71 (m, 3H), 4.50–4.33 (m, 1H), 3.95 (dd, *J*_{H,H} = 11, 3.7 Hz, 1H), 3.90–3.70 (m, 9H), 3.67 (dd, *J*_{H,H} = 12, 3.2 Hz, 1H), 3.51 (td, *J*_{H,H} = 12, 3.0 Hz, 1H), 3.26 (td, *J*_{H,H} = 13, 3.8 Hz, 1H), 1.31 (d, ³J_{H,H} = 6.8 Hz, 3H). ¹⁹F{¹H} NMR (376 MHz, CDCl₃): δ -59.9 (s, 3F). ¹³C{¹H} NMR (101 MHz, CDCl₃): δ 170.0 (s, 1C), 164.9 (s, 1C), 164.5 (s, 1C), 159.6 (s, 1C), 152.9 (s, 1C), 138.5 (q, ²J_{C,F} = 33 Hz, 1C), 123.0 (q, ¹J_{C,F} = 274 Hz, 1C), 122.6 (s, 1C), 105.4 (q, ³J_{C,F} = 4.9 Hz, 1C), 71.2 (s, 1C), 67.2 (s, 1C), 66.9 (br s, 2C), 46.4 (s, 1C), 43.7 (br s, 2C), 38.6 (s, 1C), 14.4 (s, 1C). NSI-HRMS (*m/z*): [M + H]⁺ calcd for C₁₈H₂₃F₃N₇O₂, 426.1860; found: 426.1850. HPLC: *t_R* = 7.96 min (96.9% purity).

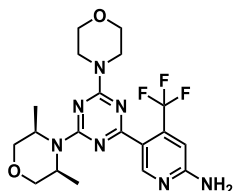


5-[4-(Morpholin-4-yl)-6-{3-oxa-8-azabicyclo[3.2.1]octan-8-yl}-1,3,5-triazin-2-yl]-4-(trifluoromethyl)pyridin-2-amine (33). Compound **33** was prepared according to general procedure 1 from intermediate **26** (80.0 mg, 257 μmol, 1.0 equiv) and boronic acid pinacol ester **48** (90.0 mg, 262 μmol, 1.0 equiv). Purification by column chromatography on silica gel (cyclohexane/ethyl acetate 1:0 → 3:7) gave compound **33** as a colorless solid (52.1 mg, 119 μmol, 46%). ¹H NMR (400 MHz, CDCl₃): δ 8.72 (s, 1H), 6.78 (s, 1H), 4.85 (br s, 2H), 4.77–4.71 (m, 1H), 4.68–4.63 (m, 1H), 3.93–3.69 (m, 10H), 3.63 (dd, ²J_{H,H} = 11 Hz, ³J_{H,H} = 1.2 Hz, 2H), 2.13–1.92 (m, 4H). ¹⁹F{¹H} NMR (376 MHz, CDCl₃): δ -59.8 (s, 3F). ¹³C{¹H} NMR (101 MHz, CDCl₃): δ 170.2 (s, 1C), 165.0 (s, 1C), 163.1 (s, 1C), 159.7 (s, 1C), 152.7 (s, 1C), 138.5 (q, ²J_{C,F} = 33 Hz, 1C), 123.0 (q, ¹J_{C,F} = 274 Hz, 1C), 122.3 (br s, 1C), 105.5 (q, ³J_{C,F} = 5.7 Hz, 1C), 72.1 (s, 1C), 71.7 (s, 1C), 66.9 (s, 2C), 54.9 (s, 1C), 54.5 (s, 1C), 43.7 (s, 2C), 27.0 (s, 2C). NSI-HRMS (*m/z*): [M + H]⁺ calcd

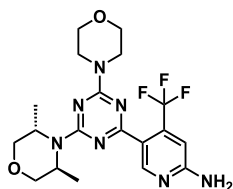
for C₁₉H₂₃F₃N₇O₂, 438.1860; found: 438.1840. HPLC: *t*_R = 7.59 min (96.6% purity).



5-[4-(Morpholin-4-yl)-6-{8-oxa-3-azabicyclo[3.2.1]octan-3-yl}-1,3,5-triazin-2-yl]-4-(trifluoromethyl)pyridin-2-amine (**34**). Compound **34** was prepared according to general procedure 1 from intermediate **27** (80.0 mg, 257 μ mol, 1.0 equiv) and boronic acid pinacol ester **48** (90.0 mg, 262 μ mol, 1.0 equiv). Purification by column chromatography on silica gel (cyclohexane/ethyl acetate 1:0 \rightarrow 3:7) gave compound **34** as a colorless solid (64.3 mg, 147 μ mol, 57%). ¹H NMR (400 MHz, CDCl₃): δ 8.70 (s, 1H), 6.77 (s, 1H), 4.91 (br s, 1H), 4.91 (br s, 2H), 4.48–4.38 (m, 3H), 4.31 (d, ²J_{H,H} = 13 Hz, 1H), 3.89–3.77 (m, 4H), 3.76–3.69 (m, 4H), 3.18 (d, ²J_{H,H} = 13 Hz, 1H), 1.98–1.87 (m, 2H), 1.82–1.72 (m, 2H). ¹⁹F{¹H} NMR (376 MHz, CDCl₃): δ -59.8 (s, 3F). ¹³C{¹H} NMR (101 MHz, CDCl₃): δ 169.8 (s, 1C), 165.9 (s, 1C), 164.7 (s, 1C), 159.6 (s, 1C), 152.8 (s, 1C), 138.5 (q, ²J_{C,F} = 33 Hz, 1C), 123.0 (q, ¹J_{C,F} = 274 Hz, 1C), 122.6–122.5 (m, 1C), 105.4 (q, ³J_{C,F} = 5.9 Hz, 1C), 74.1 (s, 1C), 74.0 (s, 1C), 66.9 (s, 2C), 49.4 (s, 1C), 49.1 (s, 1C), 43.7 (br s, 2C), 27.7 (s, 1C), 27.6 (s, 1C). NSI-HRMS (*m/z*): [M + H]⁺ calcd for C₁₉H₂₃F₃N₇O₂, 438.1860; found: 438.1851. HPLC: *t*_R = 7.46 min (99.0% purity).

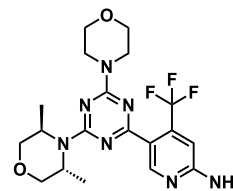


5-[4-[(3R,5S)-3,5-Dimethylmorpholin-4-yl]-6-(morpholin-4-yl)-1,3,5-triazin-2-yl]-4-(trifluoromethyl)pyridin-2-amine (**35**). Compound **35** was prepared according to general procedure 1 from intermediate **28** (200 mg, 637 μ mol, 1.0 equiv) and boronic acid pinacol ester **48** (222 mg, 647 μ mol, 1.0 equiv). Purification by column chromatography on silica gel (cyclohexane/ethyl acetate 1:0 \rightarrow 1:4) gave compound **35** as a colorless solid (60.1 mg, 137 μ mol, 21%). ¹H NMR (400 MHz, CDCl₃): δ 8.74 (s, 1H), 6.79 (s, 1H), 4.84 (br s, 2H), 4.71–4.53 (m, 2H), 3.94–3.70 (m, 10H), 3.67–3.59 (m, 2H), 1.37 (d, ³J_{H,H} = 6.9 Hz, 6H). ¹⁹F{¹H} NMR (376 MHz, CDCl₃): δ -60.2 (s, 3F). ¹³C{¹H} NMR (101 MHz, CDCl₃): δ 169.8 (s, 1C), 164.9 (s, 1C), 164.1 (s, 1C), 159.6 (s, 1C), 152.9 (s, 1C), 138.4 (q, ²J_{C,F} = 33 Hz, 1C), 123.0 (q, ¹J_{C,F} = 274 Hz, 1C), 122.5 (s, 1C), 105.8–105.0 (m, 1C), 71.5 (s, 2C), 66.9 (br s, 2C), 45.7 (s, 2C), 43.7 (br s, 2C), 19.2 (s, 2C). NSI-HRMS (*m/z*): [M + H]⁺ calcd for C₁₉H₂₅F₃N₇O₂, 440.2016; found: 440.1998. HPLC: *t*_R = 8.62 min (98.8% purity).

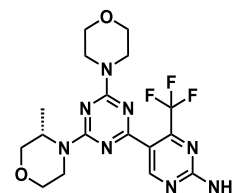


5-[4-[(3S,5S)-3,5-Dimethylmorpholin-4-yl]-6-(morpholin-4-yl)-1,3,5-triazin-2-yl]-4-(trifluoromethyl)pyridin-2-amine (**36**). Compound **36** was prepared according to general procedure 1 from intermediate **29** (200 mg, 637 μ mol, 1.0 equiv) and boronic acid pinacol ester **48** (222 mg, 647 μ mol, 1.0 equiv). Purification by column chromatography on silica gel (cyclohexane/ethyl acetate 1:0 \rightarrow 1:4) gave compound **36** as a yellowish solid (160 mg, 364 μ mol, 57%). ¹H NMR (400 MHz, CDCl₃): δ 8.75 (s, 1H), 6.79 (s, 1H), 4.84 (br s, 2H), 4.46–4.35 (m, 2H), 4.22 (dd, ²J_{H,H} = 11 Hz, ³J_{H,H} =

3.2 Hz, 2H), 3.91–3.79 (m, 4H), 3.78–3.69 (m, 6H), 1.43 (d, ³J_{H,H} = 6.6 Hz, 6H). ¹⁹F{¹H} NMR (376 MHz, CDCl₃): δ -60.2 (s, 3F). ¹³C{¹H} NMR (101 MHz, CDCl₃): δ 169.6 (s, 1C), 164.6 (s, 1C), 164.2 (s, 1C), 159.4 (s, 1C), 152.8 (s, 1C), 138.3 (q, ²J_{C,F} = 33 Hz, 1C), 122.7 (q, ¹J_{C,F} = 274 Hz, 1C), 122.5 (s, 1C), 105.3 (q, ³J_{C,F} = 6.0 Hz, 1C), 67.9 (s, 2C), 66.8 (br s, 2C), 47.9 (s, 2C), 43.6 (br s, 2C), 19.5 (s, 2C). NSI-HRMS (*m/z*): [M + H]⁺ calcd for C₁₉H₂₃F₃N₇O₂, 440.2016; found: 440.2002. HPLC: *t*_R = 8.48 min (97.5% purity).

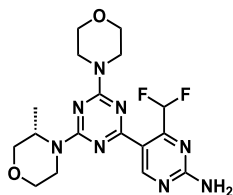


5-[4-[(3R,5R)-3,5-Dimethylmorpholin-4-yl]-6-(morpholin-4-yl)-1,3,5-triazin-2-yl]-4-(trifluoromethyl)pyridin-2-amine (**37**). Compound **37** was prepared according to general procedure 1 from intermediate **30** (175 mg, 558 μ mol, 1.0 equiv) and boronic acid pinacol ester **48** (210 mg, 612 μ mol, 1.1 equiv). Purification by column chromatography on silica gel (cyclohexane/ethyl acetate 1:0 \rightarrow 2:3) gave compound **37** as a colorless solid (111 mg, 253 μ mol, 45%). ¹H NMR (400 MHz, CDCl₃): δ 8.75 (s, 1H), 6.79 (s, 1H), 4.83 (br s, 2H), 4.47–4.34 (m, 2H), 4.22 (dd, ²J_{H,H} = 11 Hz, ³J_{H,H} = 3.4 Hz, 2H), 3.94–3.79 (m, 4H), 3.79–3.69 (m, 6H), 1.43 (d, ³J_{H,H} = 6.6 Hz, 6H). ¹⁹F{¹H} NMR (376 MHz, CDCl₃): δ -60.2 (s, 3F). ¹³C{¹H} NMR (101 MHz, CDCl₃): δ 169.7 (s, 1C), 164.7 (s, 1C), 164.4 (s, 1C), 159.6 (s, 1C), 152.9 (s, 1C), 138.4 (q, ²J_{C,F} = 33 Hz, 1C), 122.9 (q, ¹J_{C,F} = 274 Hz, 1C), 122.5 (br s, 1C), 105.4 (q, ³J_{C,F} = 5.7 Hz, 1C), 68.0 (s, 2C), 66.9 (br s, 2C), 48.0 (s, 2C), 43.7 (br s, 2C), 19.7 (s, 2C). NSI-HRMS (*m/z*): [M + H]⁺ calcd for C₁₉H₂₅F₃N₇O₂, 440.2016; found: 440.2004. HPLC: *t*_R = 8.48 min (99.2% purity).

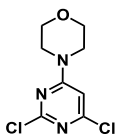


5-[4-[(3S)-3-Methylmorpholin-4-yl]-6-(morpholin-4-yl)-1,3,5-triazin-2-yl]-4-(trifluoromethyl)pyrimidin-2-amine (**38**). Intermediate **25** (100 mg, 334 μ mol, 1.0 equiv), 2-amino-4-trifluoromethylpyrimidine-5-boronic acid pinacol ester (106 mg, 367 μ mol, 1.1 equiv), phosphate tribasic (142 mg, 669 μ mol, 2.0 equiv), and chloro(2-dicyclohexylphosphino-2',4',6'-triisopropyl-1,1'-biphenyl)[2-(2'-amino-1,1'-biphenyl)]palladium(II) (XPhos Pd G2, 13.0 mg, 16.5 μ mol, 0.05 equiv) were charged in a flask. Under nitrogen atmosphere, absolute 1,4-dioxane (2.5 mL) and deionized H₂O (0.8 mL) were added and the resulting mixture was directly placed into an oil bath preheated at 95 $^{\circ}$ C and stirred at this temperature for 2 h. Then, the reaction mixture was allowed to cool down to room temperature. Brine was added and the aqueous layer was extracted with ethyl acetate (3 \times). The combined organic layer was washed with a 2 M aqueous NaOH solution, dried over anhydrous Na₂SO₄, filtered, and the solvent was rotary-evaporated under reduced pressure. The crude product was purified by column chromatography on silica gel (cyclohexane/ethyl acetate 4:1 \rightarrow 3:2) to obtain compound **38** as a colorless solid (88.2 mg, 207 μ mol, 62%). ¹H NMR (400 MHz, CDCl₃): δ 8.95 (s, 1H), 5.49 (br s, 2H), 4.84–4.67 (m, 1H), 4.50–4.32 (m, 1H), 3.95 (dd, ²J_{H,H} = 11 Hz, ³J_{H,H} = 3.4 Hz, 1H), 3.92–3.79 (m, 4H), 3.79–3.62 (m, 6H), 3.51 (td, ²J_{H,H} = 12, 2.8 Hz, 1H), 3.26 (td, ²J_{H,H} = 13, 3.8 Hz, 1H), 1.32 (d, ³J_{H,H} = 6.8 Hz, 3H). ¹⁹F{¹H} NMR (376 MHz, CDCl₃): δ -65.0 (s, 3F). ¹³C{¹H} NMR (101 MHz, CDCl₃): δ 168.5 (s, 1C), 164.8 (s, 1C), 164.4 (s, 1C), 163.1 (s, 1C), 162.7 (s, 1C), 154.5 (q, ²J_{C,F} = 35 Hz, 1C), 121.0 (s, 1C), 120.8 (q, ¹J_{C,F} = 276 Hz, 1C), 71.1 (s, 1C), 67.1 (s, 1C), 66.9 (br s, 2C), 46.5 (s, 1C), 43.7 (br s, 2C), 38.6 (s, 1C), 14.3 (br s, 1C).

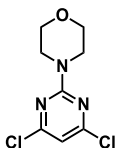
NSI-HRMS (m/z): $[M + H]^+$ calcd for $C_{17}H_{22}F_3N_8O_2$, 427.1812; found: 427.1797. HPLC: $t_R = 8.04$ min (98.5% purity).



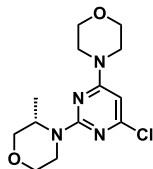
4-(Difluoromethyl)-5-{4-[(3S)-3-methylmorpholin-4-yl]-6-(morpholin-4-yl)-1,3,5-triazin-2-yl}pyrimidin-2-amine (39). Compound 39 was prepared according to general procedure 3 from intermediate 25 (100 mg, 334 μ mol, 1.1 equiv) and compound 52 (129 mg, 304 μ mol, 1.0 equiv). Purification by column chromatography on silica gel (cyclohexane/ethyl acetate 1:0 \rightarrow 3:2) gave compound 39 as a colorless solid (74.0 mg, 181 μ mol, 60%). 1H NMR (400 MHz, $CDCl_3$): δ 9.23 (s, 1H), 7.64 (t, $^2J_{H,F} = 54$ Hz, 1H), 5.65 (br s, 2H), 4.78–4.68 (m, 1H), 4.44–4.33 (m, 1H), 4.02–3.94 (m, 1H), 3.90–3.72 (m, 9H), 3.67 (dd, $^2J_{H,H} = 12$ Hz, $^3J_{H,H} = 3.3$ Hz, 1H), 3.52 (td, $J_{H,H} = 12$, 3.0 Hz, 1H), 3.34–3.21 (m, 1H), 1.33 (d, $^3J_{H,H} = 6.9$ Hz, 3H). $^{19}F\{^1H\}$ NMR (376 MHz, $CDCl_3$): δ -121.5 (s, 2F). $^{13}C\{^1H\}$ NMR (101 MHz, $CDCl_3$): δ 167.8 (s, 1C), 164.7 (s, 1C), 164.3 (s, 1C), 163.7 (s, 1C), 162.6 (s, 1C), 159.6 (t, $^2J_{C,F} = 21$ Hz, 1C), 119.8 (s, 1C), 109.6 (t, $^1J_{C,F} = 240$ Hz, 1C), 71.1 (s, 1C), 67.1 (s, 1C), 66.9 (s, 2C), 46.6 (s, 1C), 43.8 (br s, 2C), 38.7 (s, 1C), 14.4 (s, 1C). NSI-HRMS (m/z): $[M + H]^+$ calcd for $C_{17}H_{23}F_2N_8O_2$, 409.1907; found: 409.1891. HPLC: $t_R = 7.53$ min (>99.9% purity).



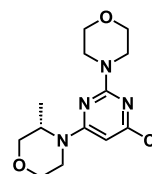
4-(2,6-Dichloropyrimidin-4-yl)morpholine (40). Compound 40 was prepared according to the literature.⁹



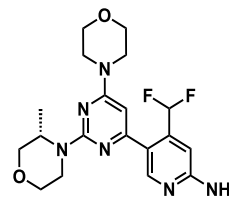
4-(4,6-Dichloropyrimidin-2-yl)morpholine (41). Compound 41 was prepared according to the literature.⁹



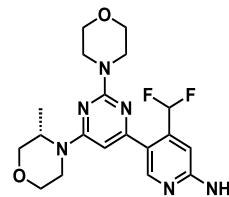
(3S)-4-[4-Chloro-6-(morpholin-4-yl)pyrimidin-2-yl]-3-methylmorpholine (42). Compound 42 was prepared according to general procedure 4 from (S)-3-methylmorpholine (450 mg, 4.45 mmol, 1.5 equiv) and 4-(2,6-dichloropyrimidin-4-yl)morpholine (40, 694 mg, 2.96 mmol, 1.0 equiv) in the presence of *N,N*-diisopropylethylamine (1.54 mL, 8.84 mmol, 3.0 equiv). Purification by column chromatography on silica gel (cyclohexane/ethyl acetate 3:1 \rightarrow 1:1) gave compound 42 as a colorless solid (475 mg, 1.59 mmol, 54%). 1H NMR (400 MHz, $CDCl_3$): δ 5.85 (s, 1H), 4.66–4.57 (m, 1H), 4.25 (dd, $J_{H,H} = 13$, 2.8 Hz, 1H), 3.93 (dd, $J_{H,H} = 11$, 3.7 Hz, 1H), 3.78–3.70 (m, 5H), 3.65 (dd, $J_{H,H} = 11$, 3.1 Hz, 1H), 3.57–3.51 (m, 4H), 3.48 (dd, $J_{H,H} = 11$, 3.0 Hz, 1H), 3.27–3.17 (m, 1H), 1.26 (d, $^3J_{H,H} = 6.8$ Hz, 3H). $^{13}C\{^1H\}$ NMR (101 MHz, $CDCl_3$): δ 163.7 (s, 1C), 160.7 (s, 1C), 160.5 (s, 1C), 91.1 (s, 1C), 71.3 (s, 1C), 67.2 (s, 1C), 66.6 (s, 2C), 46.9 (s, 1C), 44.5 (s, 2C), 39.2 (s, 1C), 13.9 (s, 1C). MALDI-MS: $m/z = 299.2$ $[M + H]^+$.



(3S)-4-[6-Chloro-2-(morpholin-4-yl)pyrimidin-4-yl]-3-methylmorpholine (43). Compound 43 was prepared according to general procedure 4 from (S)-3-methylmorpholine (194 mg, 1.92 mmol, 1.5 equiv) and 4-(4,6-dichloropyrimidin-2-yl)morpholine (41, 300 mg, 1.28 mmol, 1.0 equiv) in the presence of *N,N*-diisopropylethylamine (670 μ L, 3.84 mmol, 3.0 equiv). Purification by column chromatography on silica gel (cyclohexane/ethyl acetate 1:0 \rightarrow 4:1) gave compound 43 as a colorless solid (267 mg, 894 μ mol, 70%). 1H NMR (400 MHz, $CDCl_3$): δ 5.84 (s, 1H), 4.24–4.14 (m, 1H), 4.00–3.86 (m, 2H), 3.79–3.64 (m, 10H), 3.53 (td, $J_{H,H} = 12$, 3.1 Hz, 1H), 3.21 (td, $J_{H,H} = 13$, 3.9 Hz, 1H), 1.27 (d, $^3J_{H,H} = 6.8$ Hz, 3H). $^{13}C\{^1H\}$ NMR (101 MHz, $CDCl_3$): δ 163.0 (s, 1C), 161.0 (s, 1C), 160.6 (s, 1C), 91.2 (s, 1C), 71.0 (s, 1C), 66.9 (s, 2C), 66.8 (s, 1C), 47.4 (s, 1C), 44.4 (s, 2C), 39.3 (s, 1C), 13.7 (s, 1C). MALDI-MS: $m/z = 299.2$ $[M + H]^+$.

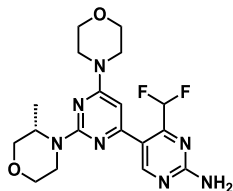


4-(Difluoromethyl)-5-{2-[(3S)-3-methylmorpholin-4-yl]-6-(morpholin-4-yl)pyrimidin-4-yl}pyridin-2-amine (44). Compound 44 was prepared according to general procedure 1 from intermediate 42 (73.5 mg, 246 μ mol, 1.0 equiv) and boronic acid pinacol ester 49 (80.0 mg, 246 μ mol, 1.0 equiv). Purification by column chromatography on silica gel (ethyl acetate/MeOH 1:0 \rightarrow 100:2) gave compound 44 as a colorless solid (57.3 mg, 141 μ mol, 57%). 1H NMR (400 MHz, $CDCl_3$): δ 8.31 (s, 1H), 7.32 (t, $^2J_{H,F} = 55$ Hz, 1H), 6.85 (s, 1H), 6.04 (s, 1H), 4.75–4.63 (m, 3H), 4.29 (dd, $^2J_{H,H} = 13$ Hz, $^3J_{H,H} = 2.1$ Hz, 1H), 3.96 (dd, $J_{H,H} = 11$, 3.4 Hz, 1H), 3.82–3.66 (m, 6H), 3.66–3.49 (m, 5H), 3.25 (td, $J_{H,H} = 13$, 3.7 Hz, 1H), 1.29 (d, $^3J_{H,H} = 6.9$ Hz, 3H). $^{19}F\{^1H\}$ NMR (376 MHz, $CDCl_3$): δ -113.7 to -117.9 (m, 2F). $^{13}C\{^1H\}$ NMR (101 MHz, $CDCl_3$): δ 163.8 (s, 1C), 162.7 (s, 1C), 161.0 (s, 1C), 159.2 (s, 1C), 149.2 (s, 1C), 142.6 (t, $^2J_{C,F} = 22$ Hz, 1C), 124.7 (t, $^3J_{C,F} = 5.2$ Hz, 1C), 111.6 (t, $^1J_{C,F} = 239$ Hz, 1C), 104.6 (t, $^3J_{C,F} = 6.9$ Hz, 1C), 91.2 (s, 1C), 71.4 (s, 1C), 67.3 (s, 1C), 66.7 (s, 2C), 46.8 (s, 1C), 44.4 (s, 2C), 39.1 (s, 1C), 13.9 (s, 1C). NSI-HRMS (m/z): $[M + H]^+$ calcd for $C_{19}H_{25}F_2N_6O_2$, 407.2002; found: 407.1989. HPLC: $t_R = 8.60$ min (97.3% purity).

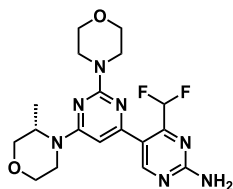


4-(Difluoromethyl)-5-{6-[(3S)-3-methylmorpholin-4-yl]-2-(morpholin-4-yl)pyrimidin-4-yl}pyridin-2-amine (45). Compound 45 was prepared according to general procedure 1 from intermediate 43 (73.5 mg, 246 μ mol, 1.0 equiv) and boronic acid pinacol ester 49 (80.0 mg, 246 μ mol, 1.0 equiv). Purification by column chromatography on silica gel (ethyl acetate/MeOH 1:0 \rightarrow 100:1) gave compound 45 as a colorless solid (74.2 mg, 183 μ mol, 74%). 1H NMR (400 MHz, $CDCl_3$): δ 8.31 (s, 1H), 7.30 (t, $^2J_{H,F} = 55$ Hz, 1H), 6.85 (s, 1H), 6.01 (s, 1H), 4.74 (br s, 2H), 4.36–4.26 (m, 1H), 4.07–3.96 (m, 1H), 3.82–3.68 (m, 11H), 3.57 (td, $J_{H,H} = 12$, 3.1 Hz, 1H), 3.24 (td, $J_{H,H} = 13$, 3.9 Hz, 1H), 1.30 (d, $^3J_{H,H} = 6.8$ Hz, 3H). $^{19}F\{^1H\}$ NMR (376 MHz, $CDCl_3$): δ -115.0 (s, 2F). $^{13}C\{^1H\}$ NMR (101 MHz, $CDCl_3$): δ 163.1 (s, 1C), 162.5 (s, 1C), 161.6 (s, 1C), 159.2 (s, 1C), 149.4 (s, 1C), 142.6 (t, $^2J_{C,F} = 22$ Hz, 1C), 124.7 (s, 1C), 111.6

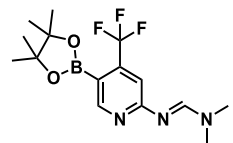
(t, $^1J_{C,F} = 239$ Hz, 1C), 104.6 (br s, 1C), 91.6 (s, 1C), 71.2 (s, 1C), 67.4–66.6 (m, 3C), 47.2 (s, 1C), 44.4 (s, 2C), 39.2 (s, 1C), 13.7 (s, 1C). NSI-HRMS (m/z): $[M + H]^+$ calcd for $C_{19}H_{25}F_2N_6O_2$, 407.2002; found: 407.1990. HPLC: $t_R = 7.65$ min (97.2% purity).



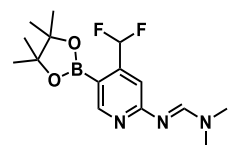
4'-(Difluoromethyl)-2-[(3S)-3-methylmorpholin-4-yl]-6-(morpholin-4-yl)-[4,5'-bipyrimidin]-2'-amine (46). Compound 46 was prepared according to general procedure 3 from intermediate 42 (101 mg, 338 μ mol, 1.1 equiv) and compound 52 (130 mg, 306 μ mol, 1.0 equiv). Purification by column chromatography on silica gel (cyclohexane/ethyl acetate 1:0 \rightarrow 3:7) gave compound 46 as a colorless solid (65.8 mg, 162 μ mol, 53%). 1H NMR (400 MHz, $CDCl_3$): δ 8.60 (s, 1H), 7.13 (t, $^2J_{H,F} = 54$ Hz, 1H), 6.01 (s, 1H), 5.41 (br s, 2H), 4.72–4.62 (m, 1H), 4.31 (dd, $^2J_{H,H} = 14$ Hz, $^3J_{H,H} = 2.2$ Hz, 1H), 3.97 (dd, $J_{H,H} = 11$, 3.4 Hz, 1H), 3.83–3.49 (m, 11H), 3.25 (td, $J_{H,H} = 13$, 3.7 Hz, 1H), 1.29 (d, $^3J_{H,H} = 6.8$ Hz, 3H). $^{19}F\{^1H\}$ NMR (376 MHz, $CDCl_3$): δ -119.9 (s, 2F). $^{13}C\{^1H\}$ NMR (101 MHz, $CDCl_3$): δ 163.7 (s, 1C), 163.0 (s, 1C), 161.0 (s, 1C), 160.4 (br s, 2C), 158.1 (t, $^2J_{C,F} = 22$ Hz, 1C), 122.6 (br s, 1C), 110.0 (t, $^1J_{C,F} = 241$ Hz, 1C), 91.1 (br s, 1C), 71.4 (s, 1C), 67.3 (s, 1C), 66.7 (s, 2C), 46.8 (s, 1C), 44.4 (s, 2C), 39.1 (s, 1C), 13.9 (s, 1C). NSI-HRMS (m/z): $[M + H]^+$ calcd for $C_{18}H_{24}F_2N_7O_2$, 408.1954; found: 408.1943. HPLC: $t_R = 7.33$ min (96.2% purity).



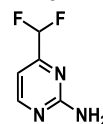
4'-(Difluoromethyl)-6-[(3S)-3-methylmorpholin-4-yl]-2-(morpholin-4-yl)-[4,5'-bipyrimidin]-2'-amine (47). Compound 47 was prepared according to general procedure 3 from intermediate 43 (101 mg, 338 μ mol, 1.1 equiv) and compound 52 (130 mg, 306 μ mol, 1.0 equiv). Purification by column chromatography on silica gel (cyclohexane/ethyl acetate 1:0 \rightarrow 1:1) gave compound 47 as a colorless solid (78.2 mg, 192 μ mol, 63%). 1H NMR (400 MHz, $CDCl_3$): δ 8.60 (s, 1H), 7.11 (t, $^2J_{H,F} = 54$ Hz, 1H), 5.99 (s, 1H), 5.40 (br s, 2H), 4.35–4.25 (m, 1H), 4.06–3.96 (m, 2H), 3.83–3.68 (m, 10H), 3.62–3.52 (m, 1H), 3.30–3.20 (m, 1H), 1.31 (d, $^3J_{H,H} = 6.3$ Hz, 3H). $^{19}F\{^1H\}$ NMR (376 MHz, $CDCl_3$): δ -119.7 (s, 2F). $^{13}C\{^1H\}$ NMR (101 MHz, $CDCl_3$): δ 163.0 (s, 1C), 162.9 (s, 1C), 161.6 (s, 1C), 160.4 (s, 1C), 160.2 (s, 1C), 158.1 (t, $^2J_{C,F} = 22$ Hz, 1C), 122.8 (br s, 1C), 110.0 (t, $^1J_{C,F} = 241$ Hz, 1C), 91.5 (s, 1C), 71.1 (s, 1C), 67.0 (s, 2C), 66.9 (s, 1C), 47.3 (s, 1C), 44.4 (s, 2C), 39.2 (s, 1C), 13.7 (s, 1C). NSI-HRMS (m/z): $[M + H]^+$ calcd for $C_{18}H_{24}F_2N_7O_2$, 408.1954; found: 408.1941. HPLC: $t_R = 6.83$ min (95.6% purity).



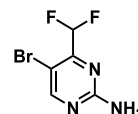
***N,N*-Dimethyl-*N'*-[5-(4,4,5,5-tetramethyl-1,3,2-dioxaborolan-2-yl)-4-(trifluoromethyl)pyridin-2-yl]methanimidamide (48).** Compound 48 was prepared according to the literature.⁹



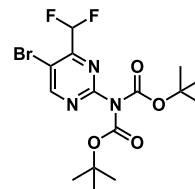
***N'*-[4-(Difluoromethyl)-5-(4,4,5,5-tetramethyl-1,3,2-dioxaborolan-2-yl)pyridin-2-yl]-*N,N*-dimethylmethanimidamide (49).** Compound 49 was prepared according to the literature.¹⁷



4-(Difluoromethyl)pyrimidin-2-amine (50). Step 1: To a solution of ethyl vinyl ether (4.00 mL, 41.8 mmol, 1.0 equiv) in a mixture of pyridine (4.10 mL, 50.7 mmol, 1.2 equiv) and dichloromethane (40 mL) at -70 $^{\circ}C$ in a dry ice/isopropyl alcohol bath, a solution of 2,2-difluoroacetic anhydride (5.90 mL, 50.1 mmol, 1.2 equiv) in dichloromethane (5 mL) was added dropwise. The resulting solution was allowed to warm up to room-temperature overnight. The mixture was then washed with deionized H_2O , the organic layer was dried over anhydrous Na_2SO_4 , filtered, and the solvent was evaporated under reduced pressure to afford an orange oil. Step 2: A solution of guanidine-HCl (4.80 g, 50.2 mmol, 1.2 equiv) in ethanol (20 mL) was stirred at room temperature for 1 h. To this solution, NaOH pellets (2.00 g, 50.0 mmol, 1.2 equiv) were added in one portion and the suspension was stirred at room temperature overnight. The above oil was diluted with dichloromethane (20 mL) and added dropwise over 1 h to the guanidine suspension. The resulting suspension was stirred at room temperature for 2 h. Dichloromethane was evaporated under reduced pressure. Deionized H_2O (25 mL) was added to the residue and the resulting mixture was stirred vigorously for 2 h and was then allowed to stand at room temperature overnight. The solid was filtered off, washed with deionized H_2O (2 \times) and heptanes (1 \times), and dried under reduced pressure. The desired product 50 was obtained as a colorless solid (3.94 g, 27.2 mmol, 65%). 1H NMR (400 MHz, $(CD_3)_2SO$): δ 8.43 (d, $^2J_{H,H} = 4.8$ Hz, 1H), 7.02 (br s, 2H), 6.76 (d, $^2J_{H,H} = 5.2$ Hz, 1H), 6.67 (t, $^2J_{H,F} = 55$ Hz, 1H). $^{19}F\{^1H\}$ NMR (376 MHz, $CDCl_3$): δ -120.5 (s, 2F). $^{13}C\{^1H\}$ NMR (101 MHz, $(CD_3)_2SO$): δ 163.5 (br s, 1C), 160.4 (s, 1C), 160.3 (t, $^2J_{C,F} = 25$ Hz, 1C), 112.6 (t, $^1J_{C,F} = 240$ Hz, 1C), 105.0 (t, $^3J_{C,F} = 4.0$ Hz, 1C).

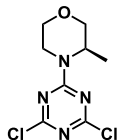


5-Bromo-4-(difluoromethyl)pyrimidin-2-amine (51). To a solution of compound 50 (3.00 g, 20.7 mmol, 1.0 equiv) in tetrahydrofuran (90 mL) at 0 $^{\circ}C$, *N*-bromosuccinimide (3.86 g, 21.7 mmol, 1.0 equiv) was added portionwise. The reaction mixture was allowed to warm up to room temperature overnight. Then, the solvent was evaporated under reduced pressure. The residue was washed with deionized H_2O (2 \times 5 mL) and cold ethyl acetate (1 \times 5 mL), and dried under reduced pressure. The desired product 51 was obtained as a yellowish solid, which was used in the next step without further purification (4.54 g, 20.3 mmol, 98% yield). 1H NMR (400 MHz, $(CD_3)_2SO$): δ 8.50 (s, 1H), 7.30 (br s, 2H), 6.87 (t, $^2J_{H,F} = 53$ Hz, 1H). $^{19}F\{^1H\}$ NMR (376 MHz, $(CD_3)_2SO$): δ -121.4 (s, 2F). $^{13}C\{^1H\}$ NMR (101 MHz, $(CD_3)_2SO$): δ 162.1 (s, 1C), 161.6 (s, 1C), 156.1 (t, $^2J_{C,F} = 23$ Hz, 1C), 112.0 (t, $^1J_{C,F} = 241$ Hz, 1C), 101.7 (s, 1C).



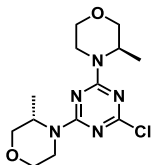
***tert*-Butyl *N*-[5-Bromo-4-(difluoromethyl)pyrimidin-2-yl]-*N*-[(*tert*-butoxy)carbonyl]carbamate (52).** To a solution of compound 51 (4.35 g, 19.4 mmol, 1.0 equiv) and 4-(dimethylamino)pyridine (480 mg, 3.92 mmol, 0.20 equiv) dissolved in tetrahydrofuran (50 mL) at 0 $^{\circ}C$, *N,N*-diisopropylethylamine (7.50 mL, 42.1 mmol, 2.2 equiv) and di-*tert*-butyl dicarbonate (9.33 g, 42.7 mmol, 2.2 equiv)

were added. The resulting solution was allowed to warm up to room temperature overnight. The solvent was evaporated under reduced pressure. The crude product was purified by column chromatography on silica gel (cyclohexane/ethyl acetate 9:1 → 4:1) to afford the desired product **52** as a colorless solid (7.00 g, 16.5 mmol, 85% yield). ^1H NMR (400 MHz, CDCl_3): δ 8.92 (s, 1H), 6.73 (t, $^2J_{\text{H,F}} = 53$ Hz, 1H), 1.47 (s, 18H). $^{19}\text{F}\{^1\text{H}\}$ NMR (376 MHz, CDCl_3): δ -120.4 (s, 2F). $^{13}\text{C}\{^1\text{H}\}$ NMR (101 MHz, CDCl_3): δ 162.6 (s, 2C), 158.1 (t, $^2J_{\text{C,F}} = 25$ Hz, 1C), 157.5 (s, 1C), 150.2 (s, 1C), 114.5 (s, 1C), 111.8 (t, $^1J_{\text{C,F}} = 244$ Hz, 1C), 84.4 (s, 2C), 27.9 (s, 6C).

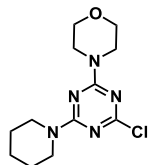


2,4-Dichloro-6-[(3R)-3-methylmorpholin-4-yl]-1,3,5-triazine (**53**).

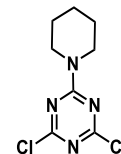
To a solution of cyanuric chloride (9.00 g, 48.8 mmol, 1.0 equiv) in dichloromethane (200 mL), a solution of *N,N*-diisopropylethylamine (8.50 mL, 48.9 mmol, 1.0 equiv) and (*R*)-3-methylmorpholine (4.90 g, 48.9 mmol, 1.0 equiv) in dichloromethane (60 mL) was slowly added at -50 °C. The mixture was stirred at -50 °C for 2 h. Aqueous saturated NaHSO_4 solution (200 mL) was added, and the resulting mixture was allowed to warm up to room temperature. The organic layer was separated, washed with aqueous saturated NaHSO_4 solution (100 mL), dried over anhydrous Na_2SO_4 , and filtered, and the solvent was evaporated under reduced pressure. The product was recrystallized from dichloromethane/heptanes to afford **53** as a colorless solid (9.30 g, 37.3 mmol, 76%). ^1H NMR (400 MHz, $(\text{CD}_3)_2\text{SO}$): δ 4.59–4.50 (m, 1H), 4.24–4.15 (m, 1H), 3.91 (dd, $J_{\text{H,H}} = 11$, 3.5 Hz, 1H), 3.69 (d, $J_{\text{H,H}} = 12$ Hz, 1H), 3.56 (dd, $J_{\text{H,H}} = 12$, 3.1 Hz, 1H), 3.46–3.25 (m, 2H), 1.26 (d, $J_{\text{H,H}} = 6.9$ Hz, 3H). $^{13}\text{C}\{^1\text{H}\}$ NMR (101 MHz, CDCl_3): δ 170.6 (s, 1C), 170.4 (s, 1C), 164.0 (s, 1C), 70.7 (s, 1C), 66.6 (s, 1C), 47.8 (s, 1C), 39.6 (s, 1C), 14.8 (s, 1C).



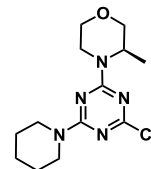
2-Chloro-4-[(3R)-3-methylmorpholin-4-yl]-6-[(3S)-3-methylmorpholin-4-yl]-1,3,5-triazine (54**).** To a solution of (*S*)-3-methylmorpholine (128 mg, 1.27 mmol, 1.1 equiv) and *N,N*-diisopropylethylamine (500 μL , 2.87 mmol, 2.4 equiv) in dichloromethane (3 mL), a solution of cyanuric chloride (300 mg, 1.20 mmol, 1.0 equiv) in dichloromethane (2 mL) was added dropwise at 0 °C in an ice bath. The resulting reaction mixture was stirred overnight, while it was allowed to warm up to room temperature. Additional dichloromethane was added and the organic layer was washed with an aqueous saturated NaHSO_4 -solution (2 \times). The organic layer was dried over anhydrous Na_2SO_4 and filtered, and the solvent was evaporated under reduced pressure. The crude product was purified by column chromatography on silica gel (cyclohexane/ethyl acetate 1:0 → 7:3) to afford compound **54** as a colorless solid (371 mg, 1.18 mmol, 99%). ^1H NMR (400 MHz, CDCl_3): δ 4.74–4.56 (m, 2H), 4.39–4.22 (m, 2H), 3.94 (dd, $J_{\text{H,H}} = 12$, 3.7 Hz, 2H), 3.73 (d, $J_{\text{H,H}} = 12$ Hz, 2H), 3.63 (dd, $J_{\text{H,H}} = 12$, 3.2 Hz, 2H), 3.48 (td, $J_{\text{H,H}} = 12$, 3.0 Hz, 2H), 3.24 (td, $J_{\text{H,H}} = 13$, 3.8 Hz, 2H), 1.30 (d, $^3J_{\text{H,H}} = 6.9$ Hz, 6H). $^{13}\text{C}\{^1\text{H}\}$ NMR (101 MHz, CDCl_3): δ 169.7 (s, 1C), 164.4 (s, 2C), 71.0 (s, 2C), 66.9 (s, 2C), 46.8 (s, 2C), 38.9 (s, 2C), 14.7 (br s, 1C), 14.3 (br s, 1C). MALDI-MS: $m/z = 313.7$ [$\text{M} + \text{H}$] $^+$.



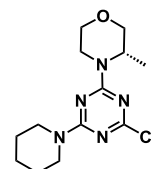
2-Chloro-4-(morpholin-4-yl)-6-(piperidin-1-yl)-1,3,5-triazine (55**).** 4-(4,6-Dichloro-1,3,5-triazin-2-yl)morpholine (23, 500 mg, 2.13 mmol, 1.0 equiv), piperidine (230 μL , 2.34 mmol, 1.1 equiv), and *N,N*-diisopropylethylamine (810 μL , 4.68 mmol, 2.2 equiv) were dissolved in ethanol (10 mL), and the resulting mixture was stirred at room temperature overnight. The solvent was then evaporated under reduced pressure, and the crude product was purified by column chromatography on silica gel (cyclohexane/ethyl acetate 1:0 → 9:1) to afford compound **55** as a colorless solid (547 mg, 1.93 mmol, 91%). The spectroscopic data are consistent with previous literature reports.³¹



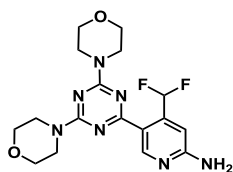
2,4-Dichloro-6-(piperidin-1-yl)-1,3,5-triazine (56**).** To a solution of cyanuric chloride (500 mg, 2.71 mmol, 1.0 equiv) in dichloromethane (12 mL), a solution of piperidine (268 μL , 2.71 mmol, 1.0 equiv) and *N,N*-diisopropylethylamine (471 μL , 2.71 mmol, 1.0 equiv) in dichloromethane (4 mL) was slowly added at -77 °C (dry ice/isopropyl alcohol bath). The resulting reaction mixture was stirred overnight, while it was allowed to warm up to room temperature. Additional dichloromethane (10 mL) was added and the organic layer was washed with an aqueous saturated NaHSO_4 solution (2 \times). The organic layer was dried over anhydrous Na_2SO_4 and filtered, and the solvent was evaporated under reduced pressure. The desired product **56** was isolated as a colorless solid and used in the next step without further purification (567 mg, 2.44 mmol, 90%). The spectroscopic data are consistent with previous literature reports.³²



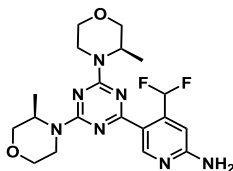
2-Chloro-4-[(3R)-3-methylmorpholin-4-yl]-6-(piperidin-1-yl)-1,3,5-triazine (57**).** 2,4-Dichloro-6-(piperidin-1-yl)-1,3,5-triazine (**56**, 180 mg, 772 μmol , 1.0 equiv), (*R*)-3-methylmorpholine (78.1 mg, 772 μmol , 1.0 equiv), and *N,N*-diisopropylethylamine (283 μL , 1.62 mmol, 2.1 equiv) were mixed in 1,4-dioxane/dichloromethane (4:1 mL), and the resulting suspension was stirred at room temperature overnight. The solvent was then evaporated under reduced pressure, and the crude product was purified by column chromatography on silica gel (cyclohexane/ethyl acetate 1:0 → 19:1) to afford compound **57** as a colorless solid (218 mg, 732 μmol , 95%). ^1H NMR (400 MHz, CDCl_3): δ 4.72–4.60 (m, 1H), 4.36–4.26 (m, 1H), 3.92 (dd, $J_{\text{H,H}} = 11$, 3.4 Hz, 1H), 3.79–3.65 (m, 5H), 3.63 (dd, $J_{\text{H,H}} = 12$, 3.0 Hz, 1H), 3.47 (td, $J_{\text{H,H}} = 12$, 2.8 Hz, 1H), 3.23 (td, $J_{\text{H,H}} = 13$, 3.8 Hz, 1H), 1.71–1.52 (m, 6H), 1.29 (d, $^3J_{\text{H,H}} = 6.9$ Hz, 3H). $^{13}\text{C}\{^1\text{H}\}$ NMR (101 MHz, CDCl_3): δ 169.7 (s, 1C), 164.4 (s, 1C), 164.2 (s, 1C), 71.0 (s, 1C), 67.0 (s, 1C), 46.7 (s, 1C), 44.6 (br s, 2C), 38.9 (s, 1C), 25.9 (br s, 1C), 25.7 (br s, 1C), 24.7 (s, 1C), 14.4 (br s, 1C). MALDI-MS: $m/z = 298.4$ [$\text{M} + \text{H}$] $^+$.



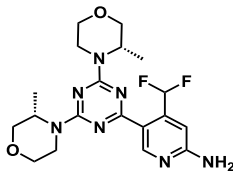
2-Chloro-4-[(3S)-3-methylmorpholin-4-yl]-6-(piperidin-1-yl)-1,3,5-triazine (58**).** Compound **58** was prepared in the same manner as its enantiomer described above, from 2,4-dichloro-6-(piperidin-1-yl)-1,3,5-triazine (**56**) and (*S*)-3-methylmorpholine in 98% yield. The spectroscopic data are in agreement with those reported for the (*R*)-enantiomer **57**.



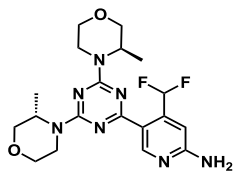
5-[4,6-Bis(morpholin-4-yl)-1,3,5-triazin-2-yl]-4-(difluoromethyl)pyridin-2-amine (**59**). Compound **59** was prepared according to the literature.¹⁷



5-[4,6-Bis((3*R*)-3-methylmorpholin-4-yl)-1,3,5-triazin-2-yl]-4-(difluoromethyl)pyridin-2-amine (**60**). Compound **60** was prepared according to general procedure 1 from intermediate **9** (250 mg, 786 μmol , 1.0 equiv) and boronic acid pinacol ester **49** (285 mg, 876 μmol , 1.1 equiv). Purification by column chromatography on silica gel (cyclohexane/ethyl acetate 1:0 \rightarrow 2:3) gave compound **60** as a colorless solid (327 mg, 776 μmol , 98%). ¹H NMR (400 MHz, CDCl₃): δ 8.97 (s, 1H), 7.70 (t, ²J_{H,F} = 55 Hz, 1H), 6.86 (s, 1H), 5.48 (br s, 2H), 4.77–4.66 (m, 2H), 4.45–4.34 (m, 2H), 3.98 (dd, J_{H,H} = 11, 3.7 Hz, 2H), 3.77 (d, J_{H,H} = 11 Hz, 2H), 3.67 (dd, J_{H,H} = 12, 3.2 Hz, 2H), 3.52 (td, J_{H,H} = 12, 3.0 Hz, 2H), 3.27 (td, J_{H,H} = 13, 3.8 Hz, 2H), 1.33 (d, ³J_{H,H} = 6.8 Hz, 6H). ¹⁹F{¹H} NMR (376 MHz, CDCl₃): δ -114.4 to -118.1 (m, 2F). ¹³C{¹H} NMR (101 MHz, CDCl₃): δ 169.3 (s, 1C), 164.5 (s, 2C), 160.2 (s, 1C), 152.5 (s, 1C), 143.7 (t, ²J_{C,F} = 22 Hz, 1C), 121.8–121.5 (m, 1C), 111.5 (t, ¹J_{C,F} = 239 Hz, 1C), 104.1 (t, ³J_{C,F} = 7.9 Hz, 1C), 71.2 (s, 2C), 67.1 (s, 2C), 46.5 (s, 2C), 38.7 (s, 2C), 14.4 (s, 2C). MALDI-MS: m/z = 421.7 [M + H]⁺. HPLC: t_R = 8.28 min (99.2% purity).

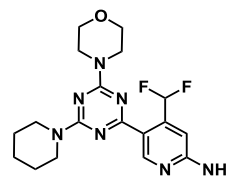


5-[4,6-Bis((3*S*)-3-methylmorpholin-4-yl)-1,3,5-triazin-2-yl]-4-(difluoromethyl)pyridin-2-amine (**61**). Compound **61** was prepared in the same manner as its enantiomer described above, from intermediate **10** and boronic acid pinacol ester **49** in 79% yield. The spectroscopic data are in agreement with those reported for the (R,R)-enantiomer **60**. HPLC: t_R = 6.39 min (95.2% purity).

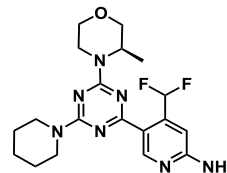


4-(Difluoromethyl)-5-[4-((3*R*)-3-methylmorpholin-4-yl)-6-((3*S*)-3-methylmorpholin-4-yl)-1,3,5-triazin-2-yl]pyridin-2-amine (**62**). Compound **62** was prepared according to general procedure 1 from intermediate **54** (271 mg, 864 μmol , 1.0 equiv) and boronic acid pinacol ester **49** (309 mg, 950 μmol , 1.1 equiv). Purification by column chromatography on silica gel (cyclohexane/ethyl acetate 1:0 \rightarrow 2:3) gave compound **62** as a colorless solid (152 mg, 361 μmol , 42%). ¹H NMR (400 MHz, CDCl₃): δ 9.04 (s, 1H), 7.69 (t, ²J_{H,F} = 55 Hz, 1H), 6.84 (s, 1H), 4.83 (br s, 2H), 4.78–4.68 (m, 2H), 4.45–4.33 (m, 2H), 3.98 (dd, J_{H,H} = 11, 3.2 Hz, 2H), 3.77 (d, J_{H,H} = 11 Hz, 2H), 3.68 (dd, J_{H,H} = 11, 2.9 Hz, 2H), 3.53 (td, J_{H,H} = 12, 2.7 Hz, 2H), 3.33–3.22 (m, 2H), 1.32 (d, ³J_{H,H} = 6.9 Hz, 6H). ¹⁹F{¹H} NMR (376 MHz, CDCl₃): δ -116.3 (s, 2F). ¹³C{¹H} NMR (101 MHz, CDCl₃): δ 169.3 (s, 1C), 164.5 (s, 2C), 160.2 (s, 1C), 152.5 (s, 1C), 143.7 (t, ²J_{C,F} = 22 Hz, 1C), 121.6 (t, ³J_{C,F} = 4.8 Hz, 1C), 111.5 (t, ¹J_{C,F} = 239 Hz, 1C), 104.1 (t, ³J_{C,F} = 7.9 Hz, 1C), 71.2 (s, 2C), 67.1

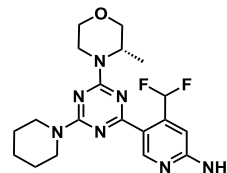
(s, 2C), 46.5 (s, 2C), 38.7 (s, 2C), 14.4 (s, 2C). MALDI-MS: m/z = 422.1 [M + H]⁺. HPLC: t_R = 8.39 min (99.5% purity).



4-(Difluoromethyl)-5-[4-(morpholin-4-yl)-6-(piperidin-1-yl)-1,3,5-triazin-2-yl]pyridin-2-amine (**63**). Compound **63** was prepared according to general procedure 1 from intermediate **55** (250 mg, 881 μmol , 1.0 equiv) and boronic acid pinacol ester **49** (301 mg, 926 μmol , 1.1 equiv). Purification by column chromatography on silica gel (cyclohexane/ethyl acetate 1:0 \rightarrow 2:3) gave compound **63** as a colorless solid (107 mg, 273 μmol , 31%). ¹H NMR (400 MHz, CDCl₃): δ 9.02 (s, 1H), 7.69 (t, ²J_{H,F} = 55 Hz, 1H), 6.83 (s, 1H), 4.83 (br s, 2H), 3.87–3.71 (m, 12H), 1.73–1.64 (m, 2H), 1.64–1.55 (m, 4H). ¹⁹F{¹H} NMR (376 MHz, CDCl₃): δ -116.2 (s, 2F). ¹³C{¹H} NMR (101 MHz, CDCl₃): δ 169.2 (s, 1C), 165.0 (s, 1C), 164.4 (s, 1C), 160.1 (s, 1C), 152.3 (s, 1C), 143.7 (t, ²J_{C,F} = 22 Hz, 1C), 122.0 (t, ³J_{C,F} = 5.0 Hz, 1C), 111.5 (t, ¹J_{C,F} = 239 Hz, 1C), 104.1 (t, ³J_{C,F} = 7.8 Hz, 1C), 67.0 (s, 2C), 44.4 (s, 1C), 43.7 (s, 2C), 25.9 (s, 2C), 25.0 (s, 2C). MALDI-MS: m/z = 392.5 [M + H]⁺. HPLC: t_R = 9.20 min (96.7% purity).



4-(Difluoromethyl)-5-[4-((3*R*)-3-methylmorpholin-4-yl)-6-(piperidin-1-yl)-1,3,5-triazin-2-yl]pyridin-2-amine (**64**). Compound **64** was prepared according to general procedure 1 from intermediate **57** (139 mg, 466 μmol , 1.0 equiv) and boronic acid pinacol ester **49** (152 mg, 467 μmol , 1.0 equiv). Purification by column chromatography on silica gel (cyclohexane/ethyl acetate 1:0 \rightarrow 2:3) gave compound **64** as a colorless solid (78.5 mg, 194 μmol , 41%). ¹H NMR (400 MHz, CDCl₃): δ 9.03 (s, 1H), 7.71 (t, ²J_{H,F} = 55 Hz, 1H), 6.83 (s, 1H), 4.82 (br s, 2H), 4.78–4.69 (m, 1H), 4.45–4.36 (m, 1H), 3.97 (dd, J_{H,H} = 11, 3.4 Hz, 1H), 3.86–3.72 (m, 5H), 3.68 (dd, J_{H,H} = 11, 3.0 Hz, 1H), 3.53 (td, J_{H,H} = 12, 2.9 Hz, 1H), 3.26 (td, J_{H,H} = 13, 3.7 Hz, 1H), 1.73–1.54 (8m, 6H), 1.32 (d, ³J_{H,H} = 6.8 Hz, 3H). ¹⁹F{¹H} NMR (376 MHz, CDCl₃): δ -115.3 to -117.5 (m, 2F). ¹³C{¹H} NMR (101 MHz, CDCl₃): δ 169.2 (s, 1C), 164.6 (s, 1C), 164.4 (s, 1C), 160.1 (s, 1C), 152.3 (s, 1C), 143.6 (t, ²J_{C,F} = 22 Hz, 1C), 122.0 (t, ³J_{C,F} = 4.9 Hz, 1C), 111.5 (t, ¹J_{C,F} = 239 Hz, 1C), 104.1 (t, ³J_{C,F} = 7.8 Hz, 1C), 71.2 (s, 1C), 67.2 (s, 1C), 46.4 (s, 1C), 44.4 (br s, 2C), 38.6 (s, 1C), 25.9 (br s, 2C), 25.0 (s, 1C), 14.3 (s, 1C). MALDI-MS: m/z = 406.3 [M + H]⁺. HPLC: t_R = 9.74 min (98.9% purity).



4-(Difluoromethyl)-5-[4-((3*S*)-3-methylmorpholin-4-yl)-6-(piperidin-1-yl)-1,3,5-triazin-2-yl]pyridin-2-amine (**65**). Compound **65** was prepared in the same manner as its enantiomer described above, from intermediate **58** and boronic acid pinacol ester **49** in 46% yield. The spectroscopic data are in agreement with those reported for the (R)-enantiomer **64**. HPLC: t_R = 9.75 min (99.0% purity).

Cellular PI3K and mTOR Signaling. Protein phosphorylation was detected as follows: pSer473 of PKB/Akt with rabbit polyclonal antibody from Cell Signaling Technology (CST) (#4058); pSer235/236 on the ribosomal protein S6 (pS6RP) with rabbit monoclonal antibody from CST (#4856) by In-Cell Western assays, where 2 \times

10^4 A2058 or 1.6×10^4 SKOV3 cells/well in 96-well plates were plated (Cell Carrier, PerkinElmer) for 24 h (37 °C, 5%CO₂). Inhibitors were incubated for 1 h before cells were fixed (4% paraformaldehyde (PFA) in phosphate-buffered saline (PBS) for 30 min at RT), blocked (1% bovine serum albumin (BSA)/0.1% Triton X-100/5% goat serum in PBS for 30 min, RT), and stained with the above primary antibodies (1:500). Tubulin was detected with mouse anti- α -tubulin (1:2000, Sigma #T9026). Secondary antibodies were IRDye680-conjugated goat antimouse, and IRDye800-conjugated goat antirabbit antibodies from LICOR (# 926-68070 and # 926-32211, at 1:500). Fluorescence was measured on an Odyssey CLx infrared imaging scanner (LICOR). Percentage of remaining phospho substrate signals was calculated in relation to cellular tubulin. Further details and calculations are explained in ref 9. Alternatively, phosphoprotein levels were assessed in A2058 cell lysates using the MSD platform in combination with the Akt Signaling Panel II Whole Cell Lysate Kit according to the manufacturer's instructions (MSD, Maryland).

Determination of Inhibitor Dissociation Constants. Dissociation constants of compounds (K_d) for p110 α and mTOR were determined by LanthaScreen Technology (Life Technologies), as described in detail in refs 9 and 10, respectively. Briefly, the AlexaFluor647-labeled Kinase Tracer314 (#PV6087) was used for p110 α with a determined K_d of 2.2 nM at 20 nM, and for mTOR with a K_d of 19 nM used at a final concentration of 10 nM. While recombinant p110 α was N-terminally (His)₆-tagged, and combined with a biotinylated anti-(His)₆-tag antibody (2 nM, #PV6089) and LanthaScreen Eu-Streptavidin (2 nM, #PV5899), truncated mTOR (amino acids 1360-2549; #PR8683B) fused to the C-terminus of glutathione S-transferase (GST) was detected with a LanthaScreen Eu-labeled anti-GST antibody (2 nM, #PV5594). The p110 α assay buffer was composed of 50 mM N-(2-hydroxyethyl)piperazine-N'-ethanesulfonic acid (HEPES) pH 7.5, 10 mM MgCl₂, 1 mM ethylene glycol-bis(β -aminoethyl ether)-N,N,N',N'-tetraacetic acid (EGTA), and 0.01% (v/v) Brij-35, and the mTOR assay buffer contained 50 mM HEPES, 5 mM MgCl₂, 1 mM EGTA, and 0.01% Pluronic F-127. Further details and calculations are described in ref 9.

Wortmannin Competition Assay. Wortmannin binding to PI3K^{19,23} was measured as described earlier.²⁰ Briefly, recombinant p110 α /p85 α protein complex (PV4789 from Life Technologies; stock 0.37 mg/mL, 1.7 μ M) was dissolved to 50 nM in HEPES reaction buffer (50 mM HEPES, 10 mM MgCl₂, 0.01% Brij-35 pH 7.4) before inhibitors were added (5 μ M, 60 min, 37 °C). Wortmannin was subsequently supplemented to a final concentration of 200 nM, followed by incubation for 20 min on ice. After sodium dodecyl sulfate-polyacrylamide gel electrophoresis and immunoblotting (to poly(vinylidene difluoride)), wortmannin covalently bound to p110 α was detected using rabbit antiwortmannin antibodies.²⁰ PI3K p110 α protein was detected with monoclonal mouse anti-p110 α (clone U3A, donated by A. Klippel), and p85 α with our rabbit anti-p85 α antibodies (H-96-Sph1).

Purification of PI3K α Protein for Structural Studies. PI3K α (Δ ABD-LBS p110 α 105-1048) was expressed by recombinant baculovirus in Sf9 cells, purified, and initially crystallized as previously published.²⁴ In brief, p110 α was produced in *Spodoptera frugiperda* (Sf9) cells by infecting 1 L of cells at a density of 1.5×10^6 cells/mL with baculovirus encoding the kinase. After 65 h of infection at 27 °C, cells were harvested and washed with phosphate-buffered saline (PBS). The p110 α construct contained an N-terminal 2 \times Strep Tag followed by a 10 \times histidine tag and tobacco etch virus (TEV) protease cleave site. Sf9 pellets were lysed in 50 mM Tris pH 8.0, 250 mM NaCl, 0.25 mM tris(2-carboxyethyl)phosphine (TCEP), 20 mM imidazole, protease inhibitor (Protease Inhibitor Cocktail Set III, Sigma) using sonication, Triton X-100 was added to 0.5% (v/v), and lysed material was centrifuged at 20 000g (Beckman J2-21, Beckman JA-20 rotor). Supernatant was passed through a 5 μ m filter and onto a HisTrap FF Crude column preequilibrated in 50 mM Tris pH 8.0, 250 mM NaCl, 0.25 mM TCEP, and 20 mM imidazole. Protein was eluted from the column using 50 mM Tris pH 8.0, 200 mM NaCl, 0.25 mM TCEP, and 200 mM imidazole. Eluted protein was passed

through a 5.0 mL StepTrapHP column preequilibrated in 50 mM Tris pH 8.0, 250 mM NaCl, 0.25 mM TCEP, and 20 mM imidazole. The column was washed with 5.0 mL of 50 mM Tris pH 8.0, 200 mM NaCl, 0.25 mM TCEP, and 40 mM imidazole, and 5.0 mL of TEV protease (0.01 mg/L) was added to the column for overnight cleavage at 4 °C. The protein was eluted with 7.0 mL of 50 mM Tris pH 8.0, 200 mM NaCl, 0.25 mM TCEP, and 40 mM imidazole and concentrated using an Amicon 50 kDa MWCO concentrator (MilliporeSigma) to 1.0 mL. The protein was loaded onto a Superdex 200 10/300 GL Increase (GE Healthcare) in 50 mM Tris pH 8.0, 100 mM NaCl, 2% ethylene glycol (EG), and 1 mM TCEP, and protein from a single peak was collected. Protein was concentrated using an Amicon 50 kDa MWCO concentrator to 6.5 mg/mL, flash-frozen as small aliquots in liquid nitrogen, and stored at -80 °C.

Crystallography. Initial apo p110 α crystallography hits were obtained from a grid of 1 μ L hanging drops containing 0.5 μ L of protein at 5.8 mg/mL (in 50 mM Tris pH 8.0, 100 mM NaCl, 2% EG, 1 mM TCEP pH 7.5) mixed 1:1 with 0.5 μ L reservoir (poly(ethylene glycol)6000 (PEG6000) 6–12%, 0.6 M sodium formate, 0.1 M N-cyclohexyl-2-aminoethanesulfonic acid (CHES) pH 9.1–9.7, 5 mM TCEP pH 7.5) at a temperature of 18 °C. Crystals collected for diffraction were obtained from 1 μ L hanging drop containing 0.5 μ L of protein at 5.8 mg/mL with a 2-fold molar excess of AFO-30 mixed with 0.4 μ L reservoir (8% PEG6000, 0.6 M Na formate, 0.1 M CHES pH 9.5, 5 mM TCEP pH 7.5) and 0.1 μ L of 1/1000 diluted microseeds crushed from a drop of the original apo crystals. Crystals were flash-frozen in liquid nitrogen after transferring to 1 μ L of reservoir solution containing 25% (v/v) glycerol as cryoprotectant and then stored in liquid nitrogen.

Diffraction data for the PI3K crystals were collected at 100 K at beamline BL14-1 of the Stanford Synchrotron Radiation Lightsource. Data were processed using XDS.²⁵ Phases were initially obtained by molecular replacement using Phaser,²⁶ with the structure of truncated PI3K α (PDB ID: 4TUU²⁴). Iterative model building and refinement were performed in COOT²⁷ and phenix.refine,²⁸ with a final $R_{\text{work}} = 24.2$ and $R_{\text{free}} = 28.7$ for the PI3K α structure bound to PQR530. Refinement was carried out with rigid body refinement, followed by translation/libration/screw B-factor and xyz refinement. The final model was verified in Molprobity for the absence of both Ramachandran and Rotamer outliers.²⁹ Data collection and refinement statistics are shown in Table S3, Supporting Information.

Structure Modeling and Determination. The X-ray structure of PQR309 (1) in PI3K γ (PDB code 5OQ4, 2.7 Å) was used as starting point. The morpholine of PQR309 (1) pointing into the hinge region of PI3K γ was substituted at the C3-position with a methyl group in (S)- and (R)-configuration. Energy minimization calculations for the resulting PI3K γ -ligand complexes were carried out. All of the four possible orientations were analyzed and superimposed. For mTOR kinase, the 3.6 Å resolution X-ray structure of PI103 in mTOR (PDB code 4JT6) was exploited as a starting point. PI103 was substituted for PQR530 (6) and its (R)-enantiomer (66). In analogy to PI3K, the two possible orientations of PQR530 (6) and 66 were analyzed and superimposed. Further measurements and figures were generated in Maestro11.1, as described in ref 17.

Kinome Profiling. The inhibitory capacity and selectivity of compound were determined using the ScanMax platform provided by DiscoverX.¹⁶ In short, binding of immobilized ligand to DNA-tagged kinases was competed with 10 μ M compound. The amount of kinase bound to the immobilized ligand was measured by quantitative PCR of the respective DNA tags and is given as percentage of control. Binding constants of compounds for kinases of interest were determined by competing the immobilized ligand kinase interactions with an 11-point threefold serial dilution of compound starting from 30 μ M and subsequent quantitative PCR of DNA tags. Binding constants were calculated by a standard dose-response curve using the Hill equation (with Hill slope set to -1)

$$\text{response} = \text{background} + (\text{signal} - \text{background}) / (1 + 10^{([\text{lg}K_d - \text{lg dose}] \times \text{Hill slope})})$$

Selectivity scores³⁰ were calculated as

$$S = \text{number of hits/number of tested kinases} \\ (\text{excluding mutant variants})$$

where $S(35)$, $S(10)$, and $S(1)$ were calculated using %Ctrl as a potency threshold (35, 10, and 1%, respectively); for example

$$S(35) = (\text{number of non-mutant kinases with \%Ctrl} \\ < 35)/(\text{number of non-mutant kinases tested})$$

Viability Studies—66 Cancer Cell Line Panel. The NTRC Oncolines 66 cell lines were exposed for 72 h to nine-point 3.16-fold serial dilutions of PQR530 (**6**), as described in refs 9 and 10. The IC_{50} 's were calculated by nonlinear regression using IDBS XLfit 5. The percentage growth after 72 h (%growth) was normalized as follows

$$100\% \times (\text{luminescence}_{t=72 \text{ h}}/\text{luminescence}_{\text{untreated}, t=72 \text{ h}})$$

This was fitted to a four-parameter logistics curve

$$\% \text{growth} = \text{bottom} + (\text{top} - \text{bottom}) \\ (1 + 10^{[(\text{Log } IC_{50} - \text{Log } x) \times \text{Hill slope}]})^{-1})$$

where bottom and top are the asymptotic minimum and maximum cell growth that the compound allows in that assay, respectively.

The LD_{50} , the concentration at which 50% of cells die, is the concentration where

$$\text{luminescence}_{t=72 \text{ h}} = \frac{1}{2} \times \text{luminescence}_{t=0 \text{ h}}$$

The GI_{50} , the concentration of 50% growth inhibition, is the concentration where cell growth is half-maximum. This is concentration associated with the signal

$$((\text{luminescence}_{\text{untreated}, t=72 \text{ h}} - \text{luminescence}_{t=0})/2) \\ + \text{luminescence}_{t=0}$$

Cell Proliferation Assays. A2058 and SKOV3 cell proliferation assays were performed as described in ref 9. Briefly, cells were seeded in 95 μL of complete Dulbecco's modified Eagle's medium (DMEM) to 96-well plates (Cell Carrier; PerkinElmer) 24 h before inhibitor treatment (5–0.02 μM for 72 h). Fixation was achieved by the addition of 65 μL of 10% paraformaldehyde (PFA) in PBS for 30 min (RT). Hoechst33324 staining was followed by addition of 1:10 volume of 1% BSA/1% Triton X-100, 10 mg/mL Hoechst33324 in PBS (30 min, RT). Fluorescent images were acquired with an Operetta High-Content System (PerkinElmer). A total of 35 fields of view were acquired per well [20 \times WD objective, with a Hoechst33324 compatible filter combination (excitation 380/20 nm, 405 nm dichroic mirror, emission 445/70 nm)].

Formulation of Compounds for in Vivo Experiments. Compound **6** (6.25 mg) were dissolved in DMSO (0.25 mL) by vortexing and sonication. After the addition of 2.25 mL of 20% hydroxypropyl- β -cyclodextrin/water, the mixture was vortexed and sonicated to get 2.5 mL of dosing solution. Formulations were homogenous at the time of application.

OVCAR-3 Xenograft Mouse Tumor Model. OVCAR-3 Cell Culture. Cells were cultured as monolayer in DMEM supplemented with 10% fetal bovine serum at 37 $^{\circ}\text{C}$ and 5% CO_2 . The cells were passaged by trypsin–ethylenediaminetetraacetic acid treatment and harvested in the exponential growth phase tumor inoculation.

Tumor Inoculation and Group Assignments. Each mouse (female BALB/c nude; age: 8–9 weeks) was inoculated subcutaneously with 5×10^6 cells (in 0.1 mL PBS) into the right flank. At treatment start, mean tumor size was ca. 157 mm^3 , body weight and tumor volume were assessed, and randomized groups using a randomized block design based on tumor volumes were established. Tumor cell inoculation is depicted as day 0.

Data Collection and Termination. Animals were monitored daily for mobility, visual estimation of food and water consumption, eye/hair matting, morbidity, mortality, tumor growth, and potential macroscopic adverse effects of drug treatment. Body weight and tumor volumes were determined three times weekly. The latter was determined in two dimensions using a caliper, and the volume was expressed in mm^3 using the formula

$$V = 0.5 \times a \times b^2$$

where a and b are the long and short diameters of the tumor, respectively. All mice were terminated on day 45 after the tumor inoculation, when the excised tumor was weighted. BALB/c nude mice were from Shanghai Lingchang Bio-Technology Co. Ltd.

Ethic Statement. All animal procedures were approved by the Institutional Animal Care and Use Committee of CrownBio. Care and use of animals was in accordance with the regulations of the Association for Assessment and Accreditation of Laboratory Animal Care.

■ ASSOCIATED CONTENT

📄 Supporting Information

The Supporting Information is available free of charge on the ACS Publications website at DOI: 10.1021/acs.jmedchem.9b00525.

Affinity of compound **6**, selected PI3K and mTOR inhibitors to PI3K and related kinases (Table S1); compounds investigating binding mode of **6** in PI3K and mTOR (Table S2); X-ray structure of compound **6** (Figure S1); X-ray crystallography data collection and refinement statistics (Table S3); modeling of **6** and compound **66** in mTOR (Figure S2); Wortmannin competition assay (Figure S3); TREEspot visualization of KINOMEScan interactions of PI3K/mTOR inhibitors (Figure S4); kinase interactions (KINOMEScan) of **6** and reference compounds (Table S4); impact on cell proliferation of **6** and GDC0980 (**3**, Table S5); cell growth dose–response curves (Figure S5); correlation of cellular growth inhibition profiles of **6**, **3**, and BEZ235 (Figure S6); comparison of PQR530 (**6**) and PQR309 (**5**) efficacies on cell viability (Figure S7); comparison of PQR530 (**6**) and PQR309 (**5**) and comparative PK in mice (Figure S8); in vitro pharmacology I–ligand binding assays with **6** (10 μM ; Table S6); in vitro pharmacology II–enzyme assays with **6** at 10 μM (Table S7); PAMPA assay (Table S8A), MDCK permeability and sensitivity to P-gp inhibitor (cyclosporine A; Table S8B); unspecific brain tissue binding, rat (Table S8C); safety profile of compound **6** (Table S9); NMR spectra, MALDI-MS images, NSI-HRMS images, and HPLC images; collected chemical formulas; and additional references (PDF)

Molecular formula strings (CSV)

Accession Codes

The coordinates of compound PQR530 (**6**) bound to the PI3K α catalytic subunit p110 α have been deposited with PDB ID code 6OAC at wwpdb.org and rcsb.org. PDB code 5OQ4 was used for docking of compounds **6** and **66** into PI3K γ . PDB code 4JT6 was used for docking of compounds **6** and **66** into mTOR kinase.

■ AUTHOR INFORMATION

Corresponding Author

*E-mail: matthias.wymann@unibas.ch. Tel: +41 61 207 5046. Fax: +41 61 207 3566.

ORCID 

Denise Rageot: 0000-0002-2833-5481

Chiara Borsari: 0000-0002-4688-8362

Alexander M. Sele: 0000-0002-4903-7934

John E. Burke: 0000-0001-7904-9859

Matthias P. Wymann: 0000-0003-3349-4281

Author Contributions

[†]D.R. and T.B. have contributed equally to this work.

Funding

This work was supported by the Swiss Commission for Technology and Innovation (CTI) by PFLS-LS grants 14032.1, 15811.2, and 17241.1; the Stiftung für Krebsbekämpfung grant 341, Swiss National Science Foundation grants 310030_153211 and 316030_133860 (to M.P.W.), and 310030B_138659; in part by European Union's Horizon 2020 research and innovation programme under the Marie Skłodowska-Curie grant agreement 675392 (to M.P.W.); and by the Cancer Research Society grant CRS-22641 (to J.E.B.).

Notes

The authors declare the following competing financial interest(s): F.B., P. Hebeisen, P. Hillmann, and D.F. are current or past employees of PIQR Therapeutics AG, Basel; and P. Hebeisen, D.F., and M.P.W. are shareholders of PIQR Therapeutics AG.

ACKNOWLEDGMENTS

The authors thank A. Pfaltz, R.A. Ettlin, W. Dieterle, S. Mukherjee, J. Mestan, and M. Lang for advice and discussions; S. Bünger and A. Dall'Asen for technical assistance; and E. Teillet, J.-B. Langlois, A. Fournier, F. Imeri, T. Masson, and J. Schwarte for early synthetic efforts. The authors are grateful to G. Zaman and the NTRC team for help and expertise with high-content screening assays.

ABBREVIATIONS

DIPEA, *N,N*-diisopropylethylamine; PK, pharmacokinetic; PI3K, phosphoinositide 3-kinase; PTEN, phosphatase and tensin homolog; PKB/Akt, protein kinase B; mTOR, mechanistic or mammalian target of rapamycin; S6K, S6 kinase; TORC, TOR complex 1 or 2; TR-FRET, time-resolved Förster resonance energy transfer; TSC2, tuberin, tuberous sclerosis 2

REFERENCES

- (1) (a) Wymann, M. P.; Schreiner, R. Lipid signalling in disease. *Nat. Rev. Mol. Cell Biol.* **2008**, *9*, 162–176. (b) Thorpe, L. M.; Yuzugullu, H.; Zhao, J. J. PI3K in cancer: divergent roles of isoforms, modes of activation and therapeutic targeting. *Nat. Rev. Cancer* **2015**, *15*, 7–24. (c) Shimobayashi, M.; Hall, M. N. Making new contacts: the mTOR network in metabolism and signalling crosstalk. *Nat. Rev. Mol. Cell Biol.* **2014**, *15*, 155–162. (d) Saxton, R. A.; Sabatini, D. M. mTOR Signaling in growth, metabolism, and disease. *Cell* **2017**, *168*, 960–976.
- (2) Janku, F.; Yap, T. A.; Meric-Bernstam, F. Targeting the PI3K pathway in cancer: are we making headway. *Nat. Rev. Clin. Oncol.* **2018**, *15*, 273–291.
- (3) Laplante, M.; Sabatini, D. M. mTOR signaling in growth control and disease. *Cell* **2012**, *149*, 274–293.
- (4) (a) Sarbassov, D. D.; Guertin, D. A.; Ali, S. M.; Sabatini, D. M. Phosphorylation and regulation of Akt/PKB by the rictor-mTOR complex. *Science* **2005**, *307*, 1098–1101. (b) Gao, T.; Furnari, F.; Newton, A. C. PHLPP: a phosphatase that directly dephosphorylates

Akt, promotes apoptosis, and suppresses tumor growth. *Mol. Cell* **2005**, *18*, 13–24.

(5) Marone, R.; Erhart, D.; Mertz, A. C.; Bohnacker, T.; Schnell, C.; Cmiljanovic, V.; Stauffer, F.; Garcia-Echeverria, C.; Giese, B.; Maira, S. M.; Wymann, M. P. Targeting melanoma with dual phosphoinositide 3-kinase/mammalian target of rapamycin inhibitors. *Mol. Cancer Res.* **2009**, *7*, 601–613.

(6) Maira, S. M.; Stauffer, F.; Brueggen, J.; Furet, P.; Schnell, C.; Fritsch, C.; Brachmann, S.; Chene, P.; De Pover, A.; Schoemaker, K.; Fabbro, D.; Gabriel, D.; Simonen, M.; Murphy, L.; Finan, P.; Sellers, W.; Garcia-Echeverria, C. Identification and characterization of NVP-BEZ235, a new orally available dual phosphatidylinositol 3-kinase/mammalian target of rapamycin inhibitor with potent in vivo antitumor activity. *Mol. Cancer Ther.* **2008**, *7*, 1851–1863.

(7) Serra, V.; Markman, B.; Scaltriti, M.; Eichhorn, P. J.; Valero, V.; Guzman, M.; Botero, M. L.; Llouch, E.; Atzori, F.; Di Cosimo, S.; Maira, M.; Garcia-Echeverria, C.; Parra, J. L.; Arribas, J.; Baselga, J. NVP-BEZ235, a dual PI3K/mTOR inhibitor, prevents PI3K signaling and inhibits the growth of cancer cells with activating PI3K mutations. *Cancer Res.* **2008**, *68*, 8022–8030.

(8) Pongas, G.; Fojo, T. BEZ235: When promising science meets clinical reality. *Oncologist* **2016**, *21*, 1033–1034.

(9) Bohnacker, T.; Protta, A. E.; Beaufls, F.; Burke, J. E.; Melone, A.; Inglis, A. J.; Rageot, D.; Sele, A. M.; Cmiljanovic, V.; Cmiljanovic, N.; Bargsten, K.; Aher, A.; Akhmanova, A.; Díaz, J. F.; Fabbro, D.; Zvelebil, M.; Williams, R. L.; Steinmetz, M. O.; Wymann, M. P. Deconvolution of buparlisib's mechanism of action defines specific PI3K and tubulin inhibitors for therapeutic intervention. *Nat. Commun.* **2017**, *8*, No. 14683.

(10) Beaufls, F.; Cmiljanovic, N.; Cmiljanovic, V.; Bohnacker, T.; Melone, A.; Marone, R.; Jackson, E.; Zhang, X.; Sele, A.; Borsari, C.; Mestan, J.; Hebeisen, P.; Hillmann, P.; Giese, B.; Zvelebil, M.; Fabbro, D.; Williams, R. L.; Rageot, D.; Wymann, M. P. 5-(4,6-Dimorpholino-1,3,5-triazin-2-yl)-4-(trifluoromethyl)pyridin-2-amine (PQR309), a potent, brain-penetrant, orally bioavailable, pan-class I PI3K/mTOR inhibitor as clinical candidate in oncology. *J. Med. Chem.* **2017**, *60*, 7524–7538.

(11) Tarantelli, C.; Gaudio, E.; Arribas, A. J.; Kwee, I.; Hillmann, P.; Rinaldi, A.; Cascione, L.; Spriano, F.; Bernasconi, E.; Guidetti, F.; Carrassa, L.; Pittau, R. B.; Beaufls, F.; Ritschard, R.; Rageot, D.; Sele, A.; Dossena, B.; Rossi, F. M.; Zucchetto, A.; Taborelli, M.; Gattei, V.; Rossi, D.; Stathis, A.; Stussi, G.; Broggin, M.; Wymann, M. P.; Wicki, A.; Zucca, E.; Cmiljanovic, V.; Fabbro, D.; Bertoni, F. PQR309 is a novel dual PI3K/mTOR inhibitor with preclinical antitumor activity in lymphomas as a single agent and in combination therapy. *Clin. Cancer Res.* **2018**, *24*, 120–129.

(12) (a) Furet, P.; Guagnano, V.; Fairhurst, R. A.; Imbach-Weese, P.; Bruce, I.; Knapp, M.; Fritsch, C.; Blasco, F.; Blanz, J.; Aichholz, R.; Hamon, J.; Fabbro, D.; Caravatti, G. Discovery of NVP-BYL719 a potent and selective phosphatidylinositol-3 kinase alpha inhibitor selected for clinical evaluation. *Bioorg. Med. Chem. Lett.* **2013**, *23*, 3741–3748. (b) Fritsch, C.; Huang, A.; Chatenay-Rivauday, C.; Schnell, C.; Reddy, A.; Liu, M.; Kauffmann, A.; Guthy, D.; Erdmann, D.; De Pover, A.; Furet, P.; Gao, H.; Ferretti, S.; Wang, Y.; Trappe, J.; Brachmann, S. M.; Maira, S. M.; Wilson, C.; Boehm, M.; Garcia-Echeverria, C.; Chene, P.; Wiesmann, M.; Cozens, R.; Lehar, J.; Schlegel, R.; Caravatti, G.; Hofmann, F.; Sellers, W. R. Characterization of the novel and specific PI3Kalpha inhibitor NVP-BYL719 and development of the patient stratification strategy for clinical trials. *Mol. Cancer Ther.* **2014**, *13*, 1117–1129.

(13) Sutherland, D. P.; Bao, L.; Berry, M.; Castanedo, G.; Chuckwether, I.; Dotson, J.; Folks, A.; Friedman, L.; Goldsmith, R.; Gunzner, J.; Heffron, T.; Lesnick, J.; Lewis, C.; Mathieu, S.; Murray, J.; Nonomiya, J.; Pang, J.; Pegg, N.; Prior, W. W.; Rouge, L.; Salphati, L.; Sampath, D.; Tian, Q.; Tsui, V.; Wan, N. C.; Wang, S.; Wei, B.; Wiesmann, C.; Wu, P.; Zhu, B. Y.; Olivero, A. Discovery of a potent, selective, and orally available class I phosphatidylinositol 3-kinase (PI3K)/mammalian target of rapamycin (mTOR) kinase inhibitor

(GDC-0980) for the treatment of cancer. *J. Med. Chem.* **2011**, *54*, 7579–7587.

(14) Burger, M. T.; Pecchi, S.; Wagman, A.; Ni, Z. J.; Knapp, M.; Hendrickson, T.; Atallah, G.; Pfister, K.; Zhang, Y.; Bartulis, S.; Frazier, K.; Ng, S.; Smith, A.; Verhagen, J.; Haznedar, J.; Huh, K.; Iwanowicz, E.; Xin, X.; Menezes, D.; Merritt, H.; Lee, L.; Wiesmann, M.; Kaufman, S.; Crawford, K.; Chin, M.; Bussiere, D.; Shoemaker, K.; Zaror, I.; Maira, S. M.; Voliva, C. F. Identification of NVP-BKM120 as a potent, selective, orally bioavailable class I PI3 kinase inhibitor for treating cancer. *ACS Med. Chem. Lett.* **2011**, *2*, 774–779.

(15) Wicki, A.; Brown, N.; Xyrafas, A.; Bize, V.; Hawle, H.; Berardi, S.; Cmiljanović, N.; Cmiljanović, V.; Stumm, M.; Dimitrijević, S.; Herrmann, R.; Prêtre, V.; Ritschard, R.; Tzankov, A.; Hess, V.; Childs, A.; Hierro, C.; Rodon, J.; Hess, D.; Joerger, M.; von Moos, R.; Sessa, C.; Kristeleit, R. First-in human, phase I, dose-escalation pharmacokinetic and pharmacodynamic study of the oral dual PI3K and mTORC1/2 inhibitor PQR309 in patients with advanced solid tumors (SAKK 67/13). *Eur. J. Cancer* **2018**, *96*, 6–16.

(16) Fabian, M. A.; Biggs, W. H.; Treiber, D. K.; Atteridge, C. E.; Azimioara, M. D.; Benedetti, M. G.; Carter, T. A.; Ciceri, P.; Edeen, P. T.; Floyd, M.; Ford, J. M.; Galvin, M.; Gerlach, J. L.; Grotzfeld, R. M.; Herrgard, S.; Insko, D. E.; Insko, M. A.; Lai, A. G.; Lélías, J. M.; Mehta, S. A.; Milanov, Z. V.; Velasco, A. M.; Wodicka, L. M.; Patel, H. K.; Zarrinkar, P. P.; Lockhart, D. J. A small molecule-kinase interaction map for clinical kinase inhibitors. *Nat. Biotechnol.* **2005**, *23*, 329–336.

(17) Rageot, D.; Bohnacker, T.; Melone, A.; Langlois, J. B.; Borsari, C.; Hillmann, P.; Sele, A. M.; Beaufls, F.; Zvelebil, M.; Hebeisen, P.; Löscher, W.; Burke, J.; Fabbro, D.; Wymann, M. P. Discovery and preclinical characterization of 5-[4,6-Bis({3-oxa-8-azabicyclo[3.2.1]octan-8-yl})-1,3,5-triazin-2-yl]-4-(difluoromethyl)pyridin-2-amine (PQR620), a highly potent and selective mTORC1/2 inhibitor for cancer and neurological disorders. *J. Med. Chem.* **2018**, *61*, 10084–10105.

(18) Brandt, C.; Hillmann, P.; Noack, A.; Römermann, K.; Öhler, L. A.; Rageot, D.; Beaufls, F.; Melone, A.; Sele, A. M.; Wymann, M. P.; Fabbro, D.; Löscher, W. The novel, catalytic mTORC1/2 inhibitor PQR620 and the PI3K/mTORC1/2 inhibitor PQR530 effectively cross the blood-brain barrier and increase seizure threshold in a mouse model of chronic epilepsy. *Neuropharmacology* **2018**, *140*, 107–120.

(19) Arcaro, A.; Wymann, M. P. Wortmannin is a potent phosphatidylinositol 3-kinase inhibitor: the role of phosphatidylinositol 3,4,5-trisphosphate in neutrophil responses. *Biochem. J.* **1993**, *296*, 297–301.

(20) (a) Wymann, M. P.; Bulgarelli-Leva, G.; Zvelebil, M. J.; Pirola, L.; Vanhaesebroeck, B.; Waterfield, M. D.; Panayotou, G. Wortmannin inactivates phosphoinositide 3-kinase by covalent modification of Lys-802, a residue involved in the phosphate transfer reaction. *Mol. Cell. Biol.* **1996**, *16*, 1722–1733. (b) Stoyanova, S.; Bulgarelli-Leva, G.; Kirsch, C.; Hanck, T.; Klinger, R.; Wetzker, R.; Wymann, M. P. Lipid kinase and protein kinase activities of G-protein-coupled phosphoinositide 3-kinase gamma: structure-activity analysis and interactions with wortmannin. *Biochem. J.* **1997**, *324*, 489–495.

(21) Engelman, J. A.; Chen, L.; Tan, X.; Crosby, K.; Guimaraes, A. R.; Upadhyay, R.; Maira, M.; McNamara, K.; Perera, S. A.; Song, Y.; Chirieac, L. R.; Kaur, R.; Lightbown, A.; Simendinger, J.; Li, T.; Padera, R. F.; Garcia-Echeverria, C.; Weissleder, R.; Mahmood, U.; Cantley, L. C.; Wong, K. K. Effective use of PI3K and MEK inhibitors to treat mutant Kras G12D and PIK3CA H1047R murine lung cancers. *Nat. Med.* **2008**, *14*, 1351–1356.

(22) (a) Khan, K. H.; Wong, M.; Rihawi, K.; Bodla, S.; Morganstein, D.; Banerji, U.; Molife, L. R. Hyperglycemia and phosphatidylinositol 3-kinase/protein kinase B/mammalian target of rapamycin (PI3K/AKT/mTOR) inhibitors in phase I trials: incidence, predictive factors, and management. *Oncologist* **2016**, *21*, 855–860. (b) Hopkins, B. D.; Pauli, C.; Du, X.; Wang, D. G.; Li, X.; Wu, D.; Amadiume, S. C.; Goncalves, M. D.; Hodakoski, C.; Lundquist, M. R.; Bareja, R.; Ma,

Y.; Harris, E. M.; Sboner, A.; Beltran, H.; Rubin, M. A.; Mukherjee, S.; Cantley, L. C. Suppression of insulin feedback enhances the efficacy of PI3K inhibitors. *Nature* **2018**, *560*, 499–503.

(23) Thelen, M.; Wymann, M. P.; Langen, H. Wortmannin binds specifically to 1-phosphatidylinositol 3-kinase while inhibiting guanine nucleotide-binding protein-coupled receptor signaling in neutrophil leukocytes. *Proc. Natl. Acad. Sci. U.S.A.* **1994**, *91*, 4960–4964.

(24) Chen, P.; Deng, Y. L.; Bergqvist, S.; Falk, M. D.; Liu, W.; Timofeevski, S.; Brooun, A. Engineering of an isolated p110 α subunit of PI3K α permits crystallization and provides a platform for structure-based drug design. *Protein Sci.* **2014**, *23*, 1332–1340.

(25) Kabsch, W. XDS. *Acta Crystallogr., Sect. D: Biol. Crystallogr.* **2010**, *66*, 125–132.

(26) McCoy, A. J.; Grosse-Kunstleve, R. W.; Adams, P. D.; Winn, M. D.; Storoni, L. C.; Read, R. J. Phaser crystallographic software. *J. Appl. Crystallogr.* **2007**, *40*, 658–674.

(27) Emsley, P.; Lohkamp, B.; Scott, W. G.; Cowtan, K. Features and development of Coot. *Acta Crystallogr., Sect. D: Biol. Crystallogr.* **2010**, *66*, 486–501.

(28) Afonine, P. V.; Grosse-Kunstleve, R. W.; Echols, N.; Headd, J. J.; Moriarty, N. W.; Mustyakimov, M.; Terwilliger, T. C.; Urzhumtsev, A.; Zwart, P. H.; Adams, P. D. Towards automated crystallographic structure refinement with phenix.refine. *Acta Crystallogr., Sect. D: Biol. Crystallogr.* **2012**, *68*, 352–367.

(29) Chen, V. B.; Arendall, W. B.; Headd, J. J.; Keedy, D. A.; Immormino, R. M.; Kapral, G. J.; Murray, L. W.; Richardson, J. S.; Richardson, D. C. MolProbity: all-atom structure validation for macromolecular crystallography. *Acta Crystallogr., Sect. D: Biol. Crystallogr.* **2010**, *66*, 12–21.

(30) Karaman, M. W.; Herrgard, S.; Treiber, D. K.; Gallant, P.; Atteridge, C. E.; Campbell, B. T.; Chan, K. W.; Ciceri, P.; Davis, M. I.; Edeen, P. T.; Faraoni, R.; Floyd, M.; Hunt, J. P.; Lockhart, D. J.; Milanov, Z. V.; Morrison, M. J.; Pallares, G.; Patel, H. K.; Pritchard, S.; Wodicka, L. M.; Zarrinkar, P. P. A quantitative analysis of kinase inhibitor selectivity. *Nat. Biotechnol.* **2008**, *26*, 127–132.

(31) Kumar, N.; Khan, S. I.; Rawat, D. S. Synthesis and antimalarial activity evaluation of tetraoxane triazine hybrids and spiro [piperidine-4,3'-tetraoxanes]. *Helv. Chim. Acta* **2012**, *95*, 1181–1197.

(32) Kumar, A.; Srivastava, K.; Kumar, S. R.; Siddiqi, M. I.; Puri, S. K.; Sexana, J. K.; Chauhan, P. M. 4-Anilinoquinoline triazines: a novel class of hybrid antimalarial agents. *Eur. J. Med. Chem.* **2011**, *46*, 676–690.